Quantum Topol. 16 (2025), 795–830
DOI 10.4171/QT/186

Murasugi sum and extremal knot Floer homology

Zhechi Cheng, Matthew Hedden, and Sucharit Sarkar

Abstract. The aim of this paper is to study the behavior of knot Floer homology under Murasugi sum. We establish a graded version of Ni's isomorphism between the extremal knot Floer homology of Murasugi sum of two links and the tensor product of the extremal knot Floer homology groups of the two summands. We further prove that $\tau = g$ for each summand if and only if $\tau = g$ holds for the Murasugi sum (with τ and g defined appropriately for multi-component links). Some applications are presented.

1. Introduction

The *Murasugi sum* is an operation that one can perform on isotopy classes of oriented surfaces with non-empty boundary embedded in 3-manifolds. Applying it to Seifert surfaces yields an operation on isotopy classes of oriented links. As the name suggests, the operation was introduced by Murasugi [18, 19], whose motivation was a calculation of the genus of an alternating link by means of the degree of its Alexander polynomial. An important point to be made about the Murasugi sum is that it *not* a well-defined binary operation on the set of oriented links. Indeed, many essential choices are made in its definition; not only the isotopy classes of the chosen Seifert surfaces, but also the polygons embedded therein along which the sum is performed. Despite these choices, one can easily show that the coefficient of the Alexander polynomial corresponding to the first Betti number of the surfaces in question is multiplicative under Murasugi sum. Gabai later showed that Seifert genus behaves additively under Murasugi sum, extending the well-known special case of the additivity of genus under connected sum. Indeed, he showed that the Murasugi sum of two surfaces is minimal genus if and only the two summands are minimal genus [5, 6]. Note, however, that pathology arises if one considers non-minimal genus surfaces; for instance, Thompson showed that one can sum two unknots along genus one surfaces to get a trefoil or sum two figure eights to get the unknot [35], and Able and

Mathematics Subject Classification 2020: 57K18.
Keywords: Murasugi sum, knot Floer homology.

Hirasawa have recently shown that in fact *any* knot can be obtained as a Murasugi sum of *any other two* knots along (typically) non-minimal genus Seifert surfaces [1].

In light of the connections between the knot Floer homology groups and both the Alexander polynomial (through their Euler characteristic [25, 32]) and the genus (through their breadth [24]), one might wonder about the behavior of the extremal knot Floer homology under Murasugi sum. Here, "extremal" refers to the knot Floer homology group in Alexander grading given by negative the genus of the surfaces used. (Modulo a well-understood grading shift, this is isomorphic to the knot Floer homology group in Alexander grading given by the genus, a group often referred to as the "top" group) For instance, the knot Floer homology groups of a connected sum are a bigraded tensor product of those of the summands [25, Theorem 7.1]. Simple examples exploiting the non-uniqueness of Murasugi sum show that this cannot hold for general Murasugi sums and, in fact, there can be no closed formula for the knot Floer homology of the Murasugi sum of links in terms of the knot Floer homology of the summands. Despite this, it would be reasonable to conjecture that the extremal knot Floer homology of a Murasugi sum is a tensor product of the extremal terms of its summands. Ni proved that this is indeed the case for *ungraded* knot Floer homology groups with field coefficients [22, Theorems 1.1,4.5] (cf. [15, Corollary 8.8]). Since an ungraded vector space over a field is determined up to isomorphism by its dimension, this result is equivalent to saying that the rank of the extremal knot Floer homology is multiplicative under Murasugi sum. It is natural to wonder if Ni's result extends in a (Maslov) graded fashion, and our first result confirms that this is indeed the case. To state it, we define the index of a (possibly disconnected) surface R to be the quantity $\mathrm{i}(R) := \frac{|\partial R| - \chi(R)}{2}$.

Theorem 1.1. *For $i \in \{1, 2\}$, let L_i be an l_i-component oriented link and let R_i be a Seifert surface for L_i. Let $R_1 * R_2$ be a Murasugi sum of R_1 and R_2, and let $\partial(R_1 * R_2) = L = L_1 * L_2$ be the corresponding l-component oriented link. Then with $\mathbb{F}_2$-coefficients, we have a graded isomorphism*

$$\begin{aligned}&\widehat{HFK}(L, -\mathrm{i}(R_1 * R_2))[l-1]\\ &\quad\cong \widehat{HFK}(L_1, -\mathrm{i}(R_1))[l_1 - 1] \otimes \widehat{HFK}(L_2, -\mathrm{i}(R_2))[l_2 - 1].\end{aligned}$$

We should note that it is not clear how to extend Ni's argument, nor the argument using the decomposition theorem for sutured Floer homology presented by Juhász, to yield the graded statement given above (despite some effort to do so). On a superficial level, though, our proof follows the same strategy as its antecedents; namely, we find particular Heegaard diagrams adapted to Seifert surfaces and their Murasugi sum, and then analyze the resulting Floer complexes in detail. The diagrams we end up using are more specialized, however, and yield more control over the combinatorics and homotopy theoretic aspects of the associated chain complexes. This increase in control further allows us to glean some information about the rest of the knot Floer homology filtration, in the form of the following result about the integer-valued concordance invariant τ [23] (for the extension of τ to links, see [4, 13, 31]).

Theorem 1.2. *If the oriented link L is the Murasugi sum of oriented links L_1 and L_2 along minimal index Seifert surfaces, then $\tau(L_i) = g(L_i)$ for all $i \in \{1, 2\}$ if and only if $\tau(L) = g(L)$. (Here τ denotes τ_{top} from* [13] *when discussing links with more than one component.)*

A large class of links for which $\tau(L) = g(L)$ is provided so-called *strongly quasipositive* links. These links possess a Seifert surface which is properly isotopic into the 4-ball onto a piece of an algebraic curve and which therefore minimizes the smooth 4-genus. Rudolph gave a partial extension of Gabai's results to 4-genera, by showing that the Murasugi sum of oriented links along Seifert surfaces is strongly quasipositive if and only if the two summands are. Our result strengthens the resulting implications for the 4-genus.

Our results lead to topological restrictions on which link types can be expressed as Murasugi sums of others along minimal index Seifert surfaces. Some of the complexity of this problem, and the restrictions offered by our theorems, can be algebraically distilled by defining a Grothendieck group of oriented links. Recall that the Grothendieck group $K(M)$, of a commutative monoid M is the quotient of the free abelian group on the set M by the relations $[x + y] = [x] + [y]$, where on the left "+" is taken with respect to the monoidal operation and on the right within the free abelian group. While the Murasugi sum $*$ is not a monoidal operation on oriented links (relying as it does on the choice of Seifert surface and embedded $2n$-gon), we can nonetheless define a group

$$K(\text{links}, *) = \frac{\mathbb{Z}\langle\{\text{Isotopy classes of oriented links}\}\rangle}{[L_1 * L_2] = [L_1] + [L_2]}$$

which we call the *Grothendieck group of oriented links under Murasugi sum along minimal index surfaces*. It is simply the quotient of the free abelian group on the set of isotopy classes of oriented links by the relations $[L_1 * L_2] = [L_1] + [L_2]$, where $*$ denotes any Murasugi sum along any $2n$-gon in any minimal index Seifert surface for the links in question. Thus, $K(\text{links}, *)$ consists of equivalence classes of oriented links, where two links are equivalent if they become isotopic after iteratively Murasugi summing both of them with some collection $(R_1, \ldots, R_i)$ of minimal index Seifert surfaces (along any $2n$-gons embedded therein, and in any order). Fibered links, endowed with their (unique) minimal index Seifert surface, form an important class of links which is closed under Murasugi sums by Gabai's work [5] (see also [34] for the closure under plumbing). If one considers their associated Grothendieck subgroup $K(\text{fibered links}, *) < K(\text{links}, *)$, a deep theorem arising from the Giroux correspondence asserts that $K(\text{fibered links}, *) \cong \mathbb{Z} \oplus \mathbb{Z}$, generated by the positive and negative Hopf links [7]. One might hope that all links could similarly be generated by a small family, given the complexity allowed by choices of Seifert surfaces and embedded $2n$-gons.

Multiplicativity of the rank of the extremal knot Floer homology under Murasugi sum shows that $K(\text{links}, *)$ is infinitely generated. Indeed, if we consider the rank of the top group as map from the set of links to the natural numbers $\mathbb{N}^{\times}$, viewed as a multiplicative monoid, then its multiplicativity under Murasugi sums implies that this map descend to a group homomorphism $K(\text{links}, *) \to K(\mathbb{N}^{\times}) \cong \mathbb{Q}^{\times}_{>0}$. Non-trivial twist knots have top group of rank equal to the number of twists, showing that the map to $\mathbb{N}^{\times}$ is surjective, hence the map to $\mathbb{Q}^{\times}_{>0}$ is surjective as well. $K(\text{links}, *)$ is therefore infinitely generated as an abelian group. One could still hope, however, that some simple infinite family of knots such as twist knots generates all knots under Murasugi sum and de-summing. Our result dashes this hope, and indicates that $K(\text{links}, *)$ is quite complicated.

Corollary 1.3. *The Poincaré polynomial of the top group of knot Floer homology induces a homomorphism*

$$P\colon K(\text{links}, *) \to \mathbb{Q}^{\times}_{>0}(t),$$

where the codomain is the multiplicative group of rational functions in t with positive rational coefficients.

It would be interesting to identify the image of P, a problem in the realm of geography questions for knot Floer homology. In particular, we have the following natural question.

Question 1.4. *Is every Laurent polynomial with $\mathbb{N}$ coefficients realized as the Poincaré polynomial of the top group of knot Floer homology for some link in the 3-sphere?*

Obstructions for a bigraded collection of abelian groups to arise as knot Floer homology groups were obtained in [2, 14], but these place no restriction on the top group.

Despite a lack of understanding of the geography question for the top group of knot Floer homology, our results indicate that any collection of knots whose Poincaré polynomials are coprime are linearly independent in the Grothendieck group, even if their total rank is the same. In particular, the kernel of the homomorphism $\mathbb{Q}^{\times}_{>0}(t) \to \mathbb{Q}^{\times}_{>0}$ induced by setting t equal 1 intersects the image of P non-trivially. Perhaps more concretely, we have the following result.

Corollary 1.5. *Suppose the Poincaré polynomial of the top group of knot Floer homology of an oriented link $L \subset S^3$ is irreducible, viewed as a Laurent polynomial over $\mathbb{Z}$. If L is a Murasugi sum of links $L = L_1 * L_2$ along minimal index Seifert surfaces, then one of L_i is fibered.*

As another quick corollary, we can show that alternating links or, more generally, links with thin Floer homology, are far from generating all links under Murasugi sum.

Corollary 1.6. *Suppose the top group of the knot Floer homology of $L \subset S^3$ is nontrivial in more than one Maslov grading. Then L is not a Murasugi sum of alternating links nor is any link which contains L as a Murasugi summand, with all Murasugi sums taken along minimal index Seifert surfaces.*

For instance, the top group of the Kenoshita–Terasaka knot and its mutant, the Conway knot, have Poincaré polynomials given by $1 + t$, up to multiplication by t^k (with $k = 2$ for the KT knot and $k = 3$ for the Conway knot) [28, Theorems 1.1 and 1.2]. Therefore, neither can be realized as a Murasugi sum of alternating links, nor is there any way to iteratively Murasugi sum them with other links to eventually arrive at a Murasugi sum of alternating (or thin) links.

As a final corollary, our results can be used in conjunction with the literature to calculate the top group of an arbitrary cable knot.

Corollary 1.7. *Let $K_{p,q}$ be the (p,q) cable of a knot K with Seifert genus g. Then, for any $p > 0$, we have the following:*

(1) *if $q > 0$, then $\widehat{HFK}_*(K_{p,q}, pg + \frac{(p-1)(q-1)}{2}) \cong \widehat{HFK}_*(K, g)$;*

(2) *if $q < 0$, then $\widehat{HFK}_*(K_{p,q}, pg + \frac{(p-1)(q-1)}{2}) \cong \widehat{HFK}_{*-(p-1)(2g-q-1)}(K, g)$.*

The key observation, due to Neumann and Rudolph, is that $K_{p,q} \cong K_{p,\mathrm{sign}(q)} * T_{p,q}$, where $\mathrm{sign}(q)$ is ± 1 depending on whether q is positive or negative [20, Figure 4.2]. Since $T_{p,q}$ is fibered, our main result indicates that the top group of a cable knot is isomorphic to that of $K_{p,\mathrm{sign}(q)}$ shifted by the grading of the top group of the corresponding torus knot. As the latter is well known to be 0 if $q > 0$ and $\frac{(p-1)(-q-1)}{2}$ if $q < 0$, the corollary can then be deduced if the top group is known for two particular examples of $K_{p,q}$; one with q positive, and one with q negative. But the results of [8, 11] (cf. [9]) indicate that the top group of $K_{p,pn+1}$ is isomorphic to that of K and the bottom group of $K_{p,-pn+1}$ is isomorphic to that of K, provided in both cases that $n \gg 0$. Together with the symmetry between the top and bottom groups of knot Floer homology, and the observations above, the corollary follows. This is essentially the argument for the special case of fibered cable knots from [10].

We conclude this introduction by highlighting a few problems and questions raised by our work. Perhaps the most interesting and challenging is the following.

Problem 1.8. *Determine the isomorphism type of* $K(\text{links}, *)$.

Solving this would, ideally, yield an explicit presentation for $K(\text{links}, *)$ by generators and relations. Note that Gabai's work implies that the link invariant $b_1^{\min}$ obtained by minimizing the first Betti number over all Seifert surfaces for a given link, is additive under Murasugi sums. Hence, it descends to a homomorphism

$$B_1^{\min}\colon K(\text{links}, *) \to K(\mathbb{N}^+) \cong \mathbb{Z}.$$

An affirmative answer to the following question would solve the following problem.

Question 1.9. *Is the homomorphism* $P \oplus B_1^{\min}\colon K(\text{links}, *) \to \mathbb{Q}_{>0}^{\times}(t) \oplus \mathbb{Z}$ *an isomorphism?*

Note that an affirmative answer would require an affirmative answer to the geography problem raised by Question 1.4. Moreover, combined with any of the known algorithms to compute knot Floer homology (e.g., [3, 17, 30]), one would also arrive at a solution to the isomorphism problem in $K(\text{links}, *)$ and, presumably, a presentation. While we are inclined to believe the answer is no, the restriction of $P \oplus B_1^{\min}$ to the subgroup generated by fibered links *is* an isomorphism onto its image. Indeed, the image of P on the fibered subgroup is the multiplicative subgroup $\{t^n\}_{n\in\mathbb{Z}}$ and the power n associated to a given fibered link is the Hopf invariant of the 2-plane field associated to its corresponding open book decomposition (up to normalization, the Hopf invariant is equal to Rudolph's *enhancement* of the Milnor number [33]). To conclude with a more tractable question, we leave the reader with the following question

Question 1.10. *Does the Poincaré polynomial homomorphism*

$$P\colon K(\text{links}, *) \to \mathbb{Q}_{>0}^{\times}(t)$$

contain an infinite rank subgroup in the kernel of the rank homomorphism obtained by setting $t = 1$ *in the Poincaré polynomial?*

Outline. The paper is organized as follow. In Section 2, we review the knot Floer homology for links, recall the definition for Murasugi sum, construct Heegaard diagrams associated to Seifert surfaces, and describe the Murasugi sum operation in terms of Heegaard diagrams. In Section 3, we study some local isotopies on Heegaard diagrams which will largely reduce the number of generators; moreover, we prove that there is a subcomplex that remains unchanged when applying these isotopies if some technical conditions are satisfied. In Section 4, we use the simplifications from the previous section to prove the main results.

2. Heegaard diagrams adapted to Seifert surfaces

2.1. Heegaard diagrams

We begin with a quick review of Heegaard diagrams. Most of what follows extends in a straightforward manner to arbitrary closed connected oriented three-manifolds, but since we are primarily concerned with the operation of Murasugi sum in S^3 we will specialize our definitions and constructions to this situation. We begin by recalling the definition of a Heegaard diagram.

Definition 2.1. A *Heegaard diagram for* S^3 is a 4-tuple

$$\mathcal{H} = (\Sigma_{(g)}, \alpha^{(g+k-1)}, \beta^{(g+k-1)}, w^{(k)})$$

where

- $\Sigma \subset S^3$ is an oriented surface of genus g whose complement has two components, the closures of which are genus g handlebodies U_α and U_β with $\Sigma = \partial U_\alpha = -\partial U_\beta$;
- $\alpha^{(g+k-1)} = (\alpha_1, \ldots, \alpha_{g+k-1})$ (respectively, $\beta^{(g+k-1)} = (\beta_1, \ldots, \beta_{g+k-1})$) is a collection of disjoint simple closed curves on Σ, each bounding a disk in the handlebody U_α (respectively, U_β), such that $\Sigma \setminus \alpha$ (respectively, $\Sigma \setminus \beta$) has exactly k components;
- the α circles are transverse to the β circles;
- $w = (w_1, \ldots, w_k)$ is a collection of markings on Σ, such that each component of $\Sigma \setminus \alpha$ contains a w marking, and each component of $\Sigma \setminus \beta$ contains a w marking.

Unless otherwise mentioned, we will assume our Heegaard diagrams to satisfy a certain technical condition called *(weak) admissibility* [29, Definition 3.5] (cf. [27, Definition 4.10]). A *generator* is a $(g+k-1)$-tuple $x = (x_1, \ldots, x_{g+k-1})$ of points in Σ, called the *coordinates* of x, such that each α and β circle contain exactly one of the coordinates; we will denote the set of generator by $\mathcal{G}_{\mathcal{H}}$.

Let $L \subset S^3$ be an l-component link and R a Seifert surface for L, not necessarily connected. Links and Seifert surfaces will always be oriented in this paper, even if we do not mention it explicitly. We have the following notion of a diagram adapted to R [12, 15, 22, 26],

Definition 2.2. A *Heegaard diagram adapted to* R is a 6-tuple

$$\mathcal{H} = (\Sigma_{(g)}, \alpha^{(g+k-1)}, \beta^{(g+k-1)}, z^{(k)}, w^{(k)}, S)$$

satisfying

- $(\Sigma, \alpha, \beta, w)$ and $(\Sigma, \alpha, \beta, z)$ are both Heegaard diagrams for S^3;

- $S \subset \Sigma$ is an oriented surface-with-boundary which is isotopic to R in S^3;
- each generator has at most $(k - \chi(R))$ coordinates inside R;
- the $2k$ markings $z = (z_1, \ldots, z_k)$ and $w = (w_1, \ldots, w_k)$ all lie on ∂S;
- each component of ∂S contains at least one marking, and on each component of ∂S, the z markings and the w markings alternate;
- the oriented arcs in ∂S joining each z marking to the next w marking are disjoint from the α circles, and the arcs in ∂S joining each w marking to the next z marking are disjoint from the β circles.

Given a Seifert surface R for an l-component link $L \subset S^3$, we can employ the following slightly enhanced version of the algorithm from [12], or a further modification thereof, to construct a Heegaard diagram adapted to R.

Algorithm 2.3. *Adapting a Heegaard diagram to a Seifert surface $R \subset S^3$.*

(H-1) Embed a graph G with n vertices and $(n - \chi(R))$ edges in the interior of the surface R, such that R deform retracts to G. Therefore, R is isotopic to $\overline{\text{nbd}_R(G)}$, the closure of a regular neighborhood of G in R. This is essentially a band presentation of R.

(H-2) Consider $\overline{\text{nbd}_{S^3}(G)}$, the closure of a regular neighborhood of G in S^3. Although $\overline{\text{nbd}_{S^3}(G)}$ is a union of handlebodies, its complement in S^3 is usually not. Rectify this by tunneling out some one-handles from the complement and adding them to $\overline{\text{nbd}_{S^3}(G)}$, so as to get a Heegaard decomposition of S^3.

(H-3) Let U_α be the handlebody obtained from $\overline{\text{nbd}_{S^3}(G)}$ by adding these new handles, and let U_β be complementary handlebody. Let Σ be the dividing Heegaard surface, oriented as the boundary of U_α.

(H-4) Push off $\overline{\text{nbd}_R(G)}$ towards Σ to get a surface $S \subset \Sigma$ in a way so as to ensure that the orientation on S induced by R agrees with the one induced by Σ.

(H-5) Place $2k$ distinct markings $z = (z_1, \ldots, z_k)$ and $w = (w_1, \ldots, w_k)$ on ∂S such that each component of ∂S contains at least one z and w marking, and on each component of ∂S, the z markings and the w markings alternate.

(H-6) If the surface Σ has genus g, then draw $(g+k-1)$ α circles and $(g+k-1)$ β circles on $\Sigma \setminus (z \cup w)$ such that the following holds:

   (a) the α circles are disjoint from one another;

   (b) the β circles are disjoint from one another;

   (c) the α circles intersect the β circles transversally;

(d) each component of $\Sigma \setminus \alpha$ contains one z marking and one w marking;

(e) each component of $\Sigma \setminus \beta$ contains one z marking and one w marking;

(f) exactly $(k - \chi(R))$ α circles intersect S.

(H-7) From each w marking, as one travels along $-\partial S$ to the next z marking, isotope all the α circles that one encounters, by finger moves, across the z marking. Similarly, from each w marking, as one travel along ∂S to the next z marking, isotope all the β circles that one encounters, by finger moves, across the z marking.

(H-8) Finally, perform isotopies of the α circles and the β circles in $\Sigma \setminus (z \cup w)$ to make the diagram admissible.

Note that such a Heegaard diagram is indeed adapted to R. In particular, (H-6f) ensures that each generator has at most $(k - \chi(R))$ coordinates inside R.

We now spell out an explicit way of making all the choices alluded to in the previous list. The process is best understood in conjunction with an explicit example, as illustrated in Figure 2.1. At various points it will be useful to make minor alterations to these choices, but for the sake of brevity (and sanity), we will not explicitly describe all the choices made each time a Heegaard diagram is constructed.

Algorithm 2.4. *Explicit diagram adapted to a planar projection of an embedded Seifert surface $R \subset S^3$.*

(E-1) Given a Seifert surface R for an l-component link $L \subset S^3$, view it as a surface lying in $\mathbb{R}^3$. Consider a projection $\pi\colon \mathbb{R}^3 \to \mathbb{R}^2$, and assume that $\pi|_R$ is generic and the image $\pi(R)$ is connected.

(E-2) If R has n components, let G be a graph with n vertices and $(n - \chi(R))$ edges, embedded in the interior of R, such that the following holds:

(a) R deform retracts to G;

(b) the vertex v is a regular point of $\pi|_R$;

(c) $\pi|_G$ is an immersion with no triple points, and all the preimages of the double points lie in the interior of the edges.

(E-3) Let $U_\alpha = \overline{\mathrm{nbd}_{S^3}(\pi(G))}$ be a genus g handlebody and let

$$U_\beta = S^3 \setminus \mathrm{nbd}_{S^3}(\pi(G))$$

be the complementary handlebody. Let $\Sigma = \partial U_\alpha$ be the Heegaard surface.

(E-4) Designate g of the $(g + 1)$ circles in $\Sigma \cap \mathbb{R}^2$ as β circles.

(E-5) For each of the $(n - \chi(R))$ edges of G, choose a point in the image of the interior of the edge that is not a double point, and draw an α circle on Σ

which is the boundary of a normal disk to G inside $U_\alpha = \overline{\text{nbd}_{S^3}(\pi(G))}$. Draw an additional α circle near each of the $(g + \chi(R) - 1)$ double points of $\pi|_G$, such that the α circle bounds a disk in U_α near the double point, and if the disk were removed by a surgery, then U_α locally would have two components, corresponding to the two preimages of the double point, with the same crossing information.

(E-6) For each vertex v_i of G, let $p_i \in \Sigma$ be the unique point such that $\pi(p_i) = \pi(v_i)$ and $|d\pi|_\Sigma(p_i)|$ has the same sign as $|d\pi|_R(v_i)|$. Let $D_i \subset \Sigma$ be a small disk containing p_i; let $D = \bigcup_i D_i$.

(E-7) For each of the $(n - \chi(R))$ edges of G, attach a band to D lying in $\Sigma \setminus (\alpha$ circles near the double points). Choose each band so that it deformation retracts onto an arc that projects to the corresponding edge under π, and so that the surface framing of the band in Σ is same as the surface framing of the corresponding edge in R. Let $S \subset \Sigma$ be the surface obtained from D by adding the bands.

(E-8) Put $2l$ markings $z = (z_1, \dots, z_l)$ and $w = (w_1, \dots, w_l)$ on $\partial S \cap \partial D$, such that each component of ∂S contains exactly one z marking and exactly one w marking, and the l arcs $b_1, \dots, b_l \subset \partial S$, which join the w markings to the z markings, are supported inside $\partial S \cap \partial D$.

(E-9) For each disk D_i, add an α circle around all but one of the b_j's supported in D_i. This adds a total of $(l - n)$ α circles.

(E-10) For $2 \le i \le l$, add a β circles around b_i.

(E-11) Perform finger moves on the α circles, as described in (H-7), to obtain the final Heegaard diagram. One can check that the diagram thus obtained is admissible. Furthermore, since the surface S was disjoint from the $(g + \chi(R) - 1)$ α circles near the double points, see (E-7), it remains disjoint from them even after the finger moves, and consequently, it only intersects $(g + l - 1) - (g + \chi(R) - 1) = (l - \chi(R))$ α circles.

2.2. Knot Floer homology

We briefly recall the definition of the "tilde" version of Heegaard Floer homology, essentially following [29, Section 6.1], cf. [17, Proposition 2.5]. Given a Heegaard diagram for S^3, $\mathcal{H} = (\Sigma_{(g)}, \alpha^{(g+k-1)}, \beta^{(g+k-1)}, w^{(k)})$, the chain complex $\widetilde{CF}_{\mathcal{H}}$ is the $\mathbb{F}_2$-module freely generated by the elements of $\mathcal{G}_{\mathcal{H}}$.

Given generators $x, y \in \mathcal{G}_{\mathcal{H}}$, a *domain* joining them is a 2-chain D generated by the elementary regions of $\mathcal{H}$ such that $\partial(\partial D \cap \alpha) = y - x$; here, an *elementary region* is the closure of a component of $\Sigma \setminus (\alpha \cup \beta)$, and we are thinking of the generators

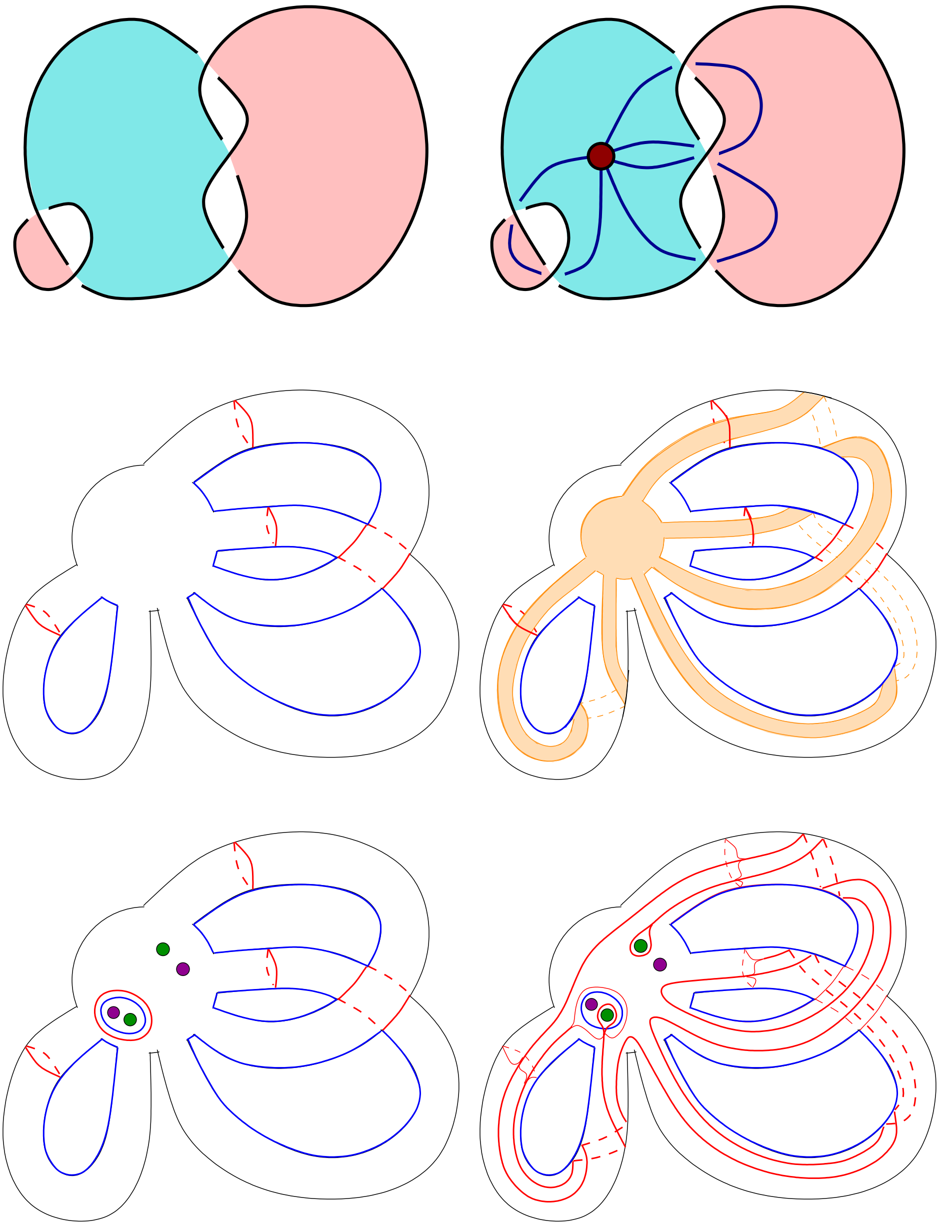

Figure 2.1. An algorithm for constructing a Heegaard diagram adapted to a Seifert surface. As usual, the red circles are α and the blue ones are β. The surface S is orange. The magenta dots are w-markings and the green dots are z-markings. In the last diagram, the α circles are represented by train tracks, with the thin red lines denoting curves.

as formal linear sums of their coordinates. The set of all the domains joining x to y is denoted by $\mathcal{D}(x, y)$. A domain D is said to be *positive* if all its coefficients are non-negative, and at least one of the coefficients is positive. Given a point $p \in \Sigma \setminus (\alpha \cup \beta)$, let $n_p(D)$ denote the coefficient of D at the elementary region containing the point p; let $n_w(D) = \sum_{i=1}^{k} n_{w_i}(D)$. Domains with $n_{w_i}(D) = 0$ for all i are called *empty domains*, and the set of all empty domains joining x to y is denoted by $\mathcal{D}_0(x, y)$. Elements of $\mathcal{G}_{\mathcal{H}}$ carry a well-defined grading called the *absolute Maslov grading* M, which serves as the homological grading of $\widetilde{CF}_{\mathcal{H}}$. The difference in Maslov gradings can be computed as

$$M(x) - M(y) = \mu(D) - 2n_w(D),$$

where $D \in \mathcal{D}(x, y)$ is any domain, and $\mu(D)$ denotes its *Maslov index.*

After choosing a generic path of almost complex structures on $\mathrm{Sym}^{g+k-1}(\Sigma)$, sufficiently close to the constant path of one induced from a complex structure on Σ, one can define the *contribution function* c, from the set of all empty Maslov index one domains, to $\mathbb{F}_2$, given by $c(D) = |\mathcal{M}(D)/\mathbb{R}|$, the number of points in a certain unparameterized moduli space. The function c has the property that it evaluates to 1 only if

(a) the domain is positive [27, Lemma 3.2], and

(b) the closure of the union of the elementary regions where the domain is supported is connected [32, Corollary 9.1].

Then the boundary map on the chain complex $\widetilde{CF}_{\mathcal{H}}$ is given by

$$\partial x = \sum_{y \in \mathcal{G}_{\mathcal{H}}} \sum_{\substack{D \in \mathcal{D}_0(x,y) \\ \mu(D)=1}} c(D) y.$$

(The chain complex $\widetilde{CF}_{\mathcal{H}}$ usually depends on the choice of the path of almost complex structures on $\mathrm{Sym}^{g+k-1}(\Sigma)$; nevertheless, we will suppress this from the notation.)

Theorem 2.5 ([17,29]). *The homology $\widetilde{HF}_{\mathcal{H}}$ of the chain complex $\widetilde{CF}_{\mathcal{H}}$ coming from a Heegaard diagram $\mathcal{H} = (\Sigma_{(g)}, \alpha^{(g+k-1)}, \beta^{(g+k-1)}, w^{(k)})$ for S^3 is isomorphic, as graded $\mathbb{F}_2$-modules, to $\otimes^{k-1}(\mathbb{F}_2 \oplus \mathbb{F}_2[-1])$, where $[i]$ denotes a grading shift by i.*

The tilde version of knot Floer homology or link Floer homology [25, 29, 32] is a refinement of Heegaard Floer homology. Let $\mathcal{H} = (\Sigma_{(g)}, \alpha^{(g+k-1)}, \beta^{(g+k-1)}, z^{(k)}, w^{(k)}, S)$ be a Heegaard diagram adapted to a Seifert surface R of an l-component link $L \subset S^3$. Consider the Heegaard diagram $\mathcal{H}_0 = (\Sigma_{(g)}, \alpha^{(g+k-1)}, \beta^{(g+k-1)}, w^{(k)})$ obtained by forgetting S and the z markings. The set of generators $\mathcal{G}_{\mathcal{H}}$ is same as $\mathcal{G}_{\mathcal{H}_0}$, and they carry the same absolute Maslov grading. Given a 2-chain D generated by the elementary regions of $\mathcal{H}$, let $n_z(D) = \sum_{i=0}^{k} n_{z_i}(D)$. The elements of $\mathcal{G}_{\mathcal{H}}$ carry another well-defined grading called the *absolute Alexander grading* A, such that for any domain $D \in \mathcal{D}(x, y)$, $A(x) - A(y) = n_z(D) - n_w(D)$.

Proposition 2.6. *If $x \in \mathcal{G}_{\mathcal{H}}$ is a generator in $\mathcal{H} = (\Sigma_{(g)}, \alpha^{(g+k-1)}, \beta^{(g+k-1)}, z^{(k)}, w^{(k)}, S)$, then its absolute Alexander grading is given by*

$$A(x) = (\textit{number of } x\textit{-coordinates inside } S) - \frac{1}{2}(2k - l - \chi(R)).$$

In particular, the Alexander grading satisfies

$$-\frac{1}{2}(2k - l - \chi(R)) \leq A(x) \leq \frac{1}{2}(l - \chi(R)).$$

Proof. The Alexander grading of a generator $x \in \mathcal{G}_{\mathcal{H}}$ is given by $\frac{1}{2}\langle c_1(s(x)), [R, \partial R]\rangle$. If the generator has no coordinate inside S (called *outer* in [15]), we can evaluate it as $\frac{1}{2}c(S)$ where $c(S)$ is the quantity defined in [15, Section 3]. Then, using [15, Lemma 3.9], we see that

$$c(S) = \chi(S) + I(S) - r(S) = \chi(S) - k - (k - l) = \chi(R) + l - 2k,$$

where $I(S)$ equals minus half the number of sutures (which are basepoints in our setting) and $r(S)$ is 0 if there is exactly one pair of sutures on each boundary and increases by one for each additional pair of sutures.

For generators which are not disjoint from S, we only need to notice that we have $c_1(s(x)) - c_1(s(y)) = 2\mathrm{PD}(\alpha)$, where $\alpha = \partial D$ for any domain $D \in \mathcal{D}(x, y)$. It is not hard to see that the algebraic intersection number of α with ∂S equals the number of x-coordinates inside S minus the number of y-coordinates inside S, and therefore,

$$A(x) = \frac{1}{2}(\chi(R) + l - 2k) + (\text{number of } x\text{-coordinates inside } S).$$

This proves the left-hand side of the inequality. For the right-hand side, we only need to use the following fact:

$$\begin{aligned}(\text{number of } x\text{-coordinates inside } S) &\leq (\text{number of } \alpha \text{ circles intersecting } S)\\ &= k - \chi(R).\end{aligned}$$

■

In view of the above proposition, we make the following definitions.

Definition 2.7. Given a compact surface R (possibly disconnected), define its *index* to be $\mathrm{i}(R) = \frac{1}{2}(|\partial R| - \chi(R))$. Call a Seifert surface R for a link L *minimal* if it minimizes the index, and define the *genus* of the link, $g(L)$, to be this minimal index.

It is easy to see that the chain complex $\widetilde{CF}_{\mathcal{H}} = \widetilde{CF}_{\mathcal{H}_0}$ is filtered by the Alexander grading. Let the filtration level $\mathcal{F}_{\mathcal{H}}(m) \subseteq \widetilde{CF}_{\mathcal{H}}$ denote the subcomplex generated by the generators with Alexander grading m or less. We call such an (M, A)-bigraded complex, where the differential decreases M by one and does not increase A, an *M-graded-A-filtered complex.*

Theorem 2.8 ([25, 29, 32]). *To an l-component link $L \subset S^3$, one can associate (the filtered chain homotopy type of) an M-graded-A-filtered complex $CFK(L)$ such that the chain complex $\widetilde{CF}_{\mathcal{H}}$, coming from any Heegaard diagram $\mathcal{H} = (\Sigma_{(g)}, \alpha^{(g+k-1)}, \beta^{(g+k-1)}, z^{(k)}, w^{(k)}, S)$ adapted to any Seifert surface R for L, is filtered chain homotopy equivalent to $CFK(L) \otimes^{k-l} (\mathbb{F}_2 \oplus \mathbb{F}_2[-1,-1])$, where $[i, j]$ denotes the (M, A) bi-grading shift by (i, j).*

It is clear from Proposition 2.6 and Theorem 2.8 that the subcomplex of $CFK(L)$ in Alexander grading less than $-\mathrm{i}(R)$ is filtered chain homotopy equivalent to zero. Let $\widehat{CFK}(L, -\mathrm{i}(R))$ denote the subcomplex of $CFK(L)$ in Alexander grading less than or equal to $-\mathrm{i}(R)$. If R is minimal, then its homology, $\widehat{HFK}(L, -g(L))$, is nonzero [21, 24] carrying a single grading coming from the Maslov grading, and is called the *extremal knot Floer homology*.

Instead of studying the full filtration on $CFK(L)$, we will restrict our attention to the two-step filtration $\widehat{CFK}(L, -\mathrm{i}(R)) \subset CFK(L)$. Recall that a *two-step filtered complex* is simply a pair (S, C) where C is a chain complex and $S \subset C$ is a subcomplex. A filtered chain map f from (S, C) to (S', C') is a chain map $f: C \to C'$ so that $f(S) \subseteq S'$. A filtered chain map f from (S, C) to (S', C') is a *quasi-isomorphism* if both $f: C \to C'$ and $f|_S: S \to S'$ induce isomorphisms on homology. We will make use of the following corollary of Theorem 2.8

Corollary 2.9. *Let $\mathcal{H} = (\Sigma_{(g)}, \alpha^{(g+k-1)}, \beta^{(g+k-1)}, z^{(k)}, w^{(k)}, S)$ be a Heegaard diagram adapted to a minimal Seifert surface R for L. Then there is a quasi-isomorphism of pairs*

$$\begin{aligned}&(\mathcal{F}_{\mathcal{H}}(-\mathrm{i}(R) - k + l), \widetilde{CF}_{\mathcal{H}})\\ &\quad \cong (\widehat{CFK}(L, -g(L)) \otimes^{k-l} (\mathbb{F}_2[-1,-1]), CFK(L) \otimes^{k-l} (\mathbb{F}_2 \oplus \mathbb{F}_2[-1,-1])).\end{aligned}$$

In particular, the extremal knot Floer homology is isomorphic to the homology of $\mathcal{F}_{\mathcal{H}}(-\mathrm{i}(R) - k + l)[k - l]$. Moreover, the maps on homologies, $\widehat{HFK}(L, -g(L)) \to H_*(CFK(L))$ and $H_*(\mathcal{F}_{\mathcal{H}}(-\mathrm{i}(R) - k + l)) \to \widetilde{HF}_{\mathcal{H}}$ have the same rank.

We conclude this section by describing how the extremal knot Floer homology is related to the τ-invariant. Ozaváth and Szabó originally defined the τ-invariant for knots in S^3; there are a number of generalizations of this invariant to links, and we will concentrate on τ_{bot} and τ_{top} which, by [13, Proposition 5.16] correspond to the smallest and largest of all the possible τ invariants for links (For a knot K, $\tau(K) = \tau_{\text{bot}}(K) = \tau_{\text{top}}(K)$.) For now, we only need the following properties of these invariants.

Proposition 2.10. *If $m(L)$ denotes the mirror of L, then $\tau_{\mathrm{bot}}(m(L)) = -\tau_{\mathrm{top}}(L)$. The invariant τ_{bot} satisfies $-g(L) \leq \tau_{\mathrm{bot}}(L) \leq g(L)$ with $\tau_{\mathrm{bot}}(L) = -g(L)$ if and only if the map $\widehat{HFK}(L, -g(L)) \to H_*(CFK(L))$ is non-zero.*

Proof. The relationship between τ_{bot} and τ_{top} under mirroring follows from their definition, a duality property satisfied by generalized τ invariants [13, Proposition 2.5]. That τ_{bot} is bounded by the genus of L follows from the fact that it is correspondingly bounded by the "slice genus" [13, Proposition 5.14]. The final statement is a consequence of the definition of τ_{bot}, and the monotonicity of the τ invariants for links established in [13, Proposition 5.16]. See [13, Theorem 2 and Section 5.3] for more details. ∎

Proposition 2.11. *Let $\mathcal{H} = (\Sigma_{(g)}, \alpha^{(g+k-1)}, \beta^{(g+k-1)}, z^{(k)}, w^{(k)}, S)$ be a Heegaard diagram adapted to a minimal Seifert surface R for a knot $L \subset S^3$. Then $\tau_{\mathrm{bot}}(L) = -g(L)$ if and only if the map on homology $H_*(\mathcal{F}_{\mathcal{H}}(-g(L) - k + l)) \to \widetilde{HF}_{\mathcal{H}}$ induced from the inclusion $\mathcal{F}_{\mathcal{H}}(-g(L) - k + l) \hookrightarrow \widetilde{CF}_{\mathcal{H}}$ is non-trivial.*

Proof. This follows immediately from Proposition 2.10 and Corollary 2.9. ∎

2.3. Triangle maps

We briefly introduce the definition of triangle maps in our restricted setting, once again following the original definitions from [27]. Let $\mathcal{H} = (\Sigma_{(g)}, \alpha^{(g+k-1)}, \beta^{(g+k-1)}, \gamma^{(g+k-1)}, w^{(k)})$ be a *triple Heegaard diagram*, that is, $\mathcal{H}_{\alpha\beta} = (\Sigma, \alpha, \beta, w)$ and $\mathcal{H}_{\gamma\beta} = (\Sigma, \gamma, \beta, w)$ are Heegaard diagrams for S^3; α_i is disjoint from γ_j for $i \neq j$; α_i is transverse to γ_i and they intersect each other in exactly two points, none of which lies on the β curves; furthermore, if α_j bounds a disk D_j in the α-handlebody U_α, then γ_i is isotopic to α_i in $\mathrm{nbd}_{U_\alpha}(\bigcup_{j\neq i} D_j) \cup (\Sigma \setminus w)$, that is, γ_i can be isotoped to α_i after sliding it over some other α circles in the complement of the w markings. We will once again assume that the triple Heegaard diagram is *admissible*.

Orient α_i arbitrarily, and then orient γ_i in the same direction, induced from the isotopy joining γ_i to α_i. Let θ_i be the positive intersection point in $\gamma_i \cap \alpha_i$, and let $\theta = (\theta_1, \ldots, \theta_{g+k-1})$. It is usually called the *top generator*. Note that $(\Sigma, \gamma, \alpha, w)$ is a Heegaard diagram for $\#^g(S^1 \times S^2)$ on which $(k-1)$ index 0/3 stabilizations have been performed, and θ is its unique generator of highest Maslov grading.

Elementary regions of $\mathcal{H}$ are closures of the components of $\Sigma \setminus (\alpha \cup \beta \cup \gamma)$; a *triangular domain* joining a generator $x \in \mathcal{G}_{\mathcal{H}_{\alpha\beta}}$ to a generator $y \in \mathcal{G}_{\mathcal{H}_{\gamma\beta}}$ is a 2-chain D generated by the elementary regions such that $\partial(\partial D \cap \alpha) = \theta - x$ and $\partial(\partial D \cap \beta) = x - y$; a triangular domain is said to be *positive* if all its coefficients are non-negative. Given a triangular domain D, let $n_w(D) = \sum_i n_{w_i}(D)$, where $n_{w_i}(D)$ is the coefficient of the elementary region containing w_i, in the 2-chain D. Let $\mathcal{T}(x, y)$

be the set of all triangular domains joining $x \in \mathcal{G}_{\mathcal{H}_{\alpha\beta}}$ to $y \in \mathcal{G}_{\mathcal{H}_{\gamma\beta}}$, and let $\mathcal{T}_0(x, y)$ be the subset consisting of the *empty triangular domains*, that is, triangular domains with $n_{w_i} = 0$ for all i. The *Maslov grading* $\mu(D)$ of any triangular domain $D \in \mathcal{T}(x, y)$ satisfies $\mu(D) - 2n_w(D) = M(y) - M(x)$.

Choosing an appropriate family (parametrized by the 2-simplex) of almost complex structures on $\mathrm{Sym}^{g+k-1}(\Sigma)$, we can define a *contribution function* c from the set of all Maslov index zero triangular domains to $\mathbb{F}_2$. Picking the family of almost complex structures to be integrable near a collection of hypersurfaces specified by basepoints in the elementary regions ensures that the contribution function has nonzero support only on the positive triangular domains. Then the following map is a graded quasi-isomorphism from $\widetilde{CF}_{\mathcal{H}_{\alpha\beta}}$ to $\widetilde{CF}_{\mathcal{H}_{\gamma\beta}}$:

$$f(x) = \sum_{y \in \mathcal{G}_{\mathcal{H}_{\gamma\beta}}} \sum_{\substack{D \in \mathcal{T}_0(x,y) \\ \mu(D)=0}} c(D) y.$$

We will reprove a special case of this fact in Theorem 3.3.

2.4. Murasugi sum

We are now prepared to discuss the Murasugi sum operation. Let $S^2 \subset S^3$ be the standard 2-sphere. We will mentally "one-point-decompactify" the picture, and draw it as $\mathbb{R}^2 \subset \mathbb{R}^3$. There are two components in $S^3 \setminus S^2$, the "inside" B_1 and the "outside" B_2, such that S^2 is oriented as ∂B_1. Let $A_1 A_2 \dots A_{2n}$ be a $2n$-gon lying on S^2. For $i \in \{1, 2\}$, let R_i be a Seifert surface for an l_i-component link $L_i \subset \overline{B_i}$, such that $R_i \cap S^2$ is $A_1 A_2 \dots A_{2n}$ with the same orientation; $L_1 \cap S^2$ is the union of the oriented segments $A_1 A_2$, $A_3 A_4$, ..., $A_{2n-1} A_{2n}$; and $L_2 \cap S^2$ is the union of the oriented segments $A_2 A_3$, $A_4 A_5$, ..., $A_{2n} A_1$. Then the *Murasugi sum* $L = L_1 * L_2$ is the link $\overline{(L_1 \cup L_2) \setminus S^2}$, and it bounds the Seifert surface $R_1 * R_2 = R_1 \cup R_2$. The special cases when $n = 1$ is just the connected sum and $n = 2$ is a plumbing. The case $n = 2$ is illustrated in Figure 2.2.

We need the following quantities, $\delta_1, \delta_2, \delta$, which will simplify certain expressions later on. Define δ_1 (respectively, δ_2, δ) to be n minus the number of components of L_1 (respectively, L_2, L) that intersect the $2n$-gon. Note, $(l + \delta - n) = (l_1 + \delta_1 - n) + (l_2 + \delta_2 - n)$.

We will now describe how to draw Heegaard diagrams adapted to R_1 and R_2, and how they can be combined to form a Heegaard diagram for $R_1 * R_2$. The procedures closely follow the outline from Section 2.1 with a few differences. The most important feature of the following construction is that the roles of α and β are reversed while constructing the Heegaard diagrams adapted to R_1 and R_2.

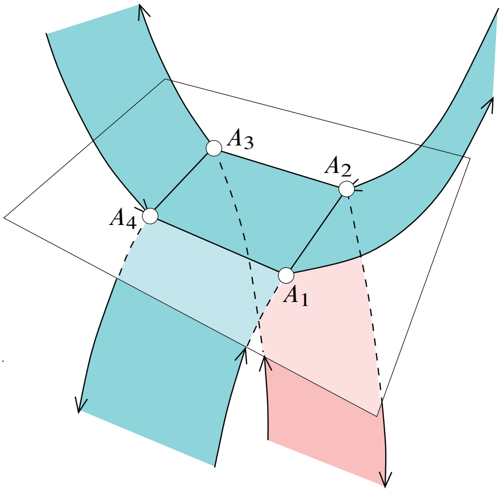

Figure 2.2. The Murasugi sum operation. The link L is obtained by plumbing the link L_1 below the plane with the link L_2 above the plane along the rectangle $A_1A_2A_3A_4$.

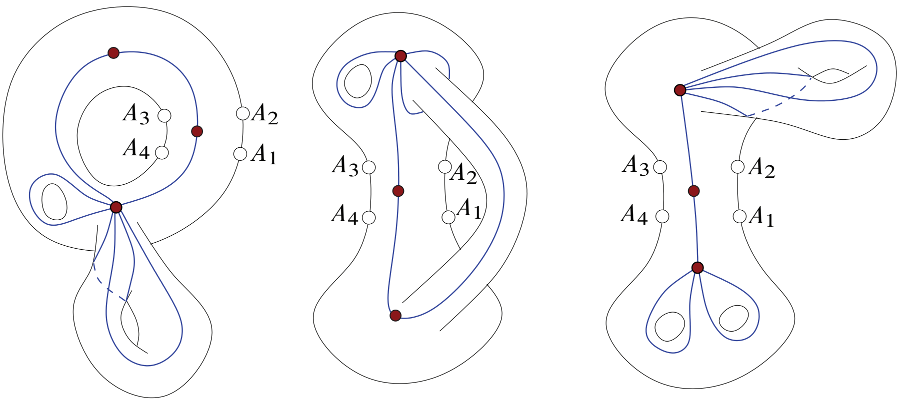

Figure 2.3. Embedding a graph G in the Seifert surface. In each case, the Seifert surface deform retracts to a neighborhood of G that contains $A_1A_2A_3A_4$.

(M-1) We first embed a graph G_i in R_i so that R_i deform retracts to G_i, and G_i intersects the $2n$-gon in a single vertex with exactly n edges going out to n of its edges. This is easy to ensure, see Figure 2.3.

(M-2) Then consider the handlebody $\overline{B_{3-i} \cup \mathrm{nbd}_{B_i}(G_i \cap B_i)}$. Its complement need not be a handlebody, so we add a few tunnels, none intersecting S^2, to complete this to a Heegaard decomposition of S^3. Let Σ_i be the resulting Heegaard surface, oriented so that its orientation agrees with the orientation of $S^2 = \partial B_1$ on $S^2 \cap \Sigma_i$. Let $U_{\alpha,i}$ and $U_{\beta,i}$ be the components of $S^3 \setminus \Sigma_i$, so that Σ_i is oriented as the boundary of $U_{\alpha,i}$.

(M-3) Construct a surface $S_i \subset \Sigma_i$, such that S_i is isotopic to R_i and $S_i \cap S^2$ is the $2n$-gon $A_1 A_2 \ldots A_{2n} \cap \Sigma_i$.

(M-4) Put z markings at $A_1, A_3, \ldots, A_{2n-1}$, and put w markings at $A_2, A_4, \ldots, A_{2n}$. On every other component of ∂S_i, put a z marking and a w marking right next to one another, such that a small arc in $(-1)^i \partial S_i$ joins the w marking to the z marking. Therefore, the total number of z (or w) markings is $l_i + \delta_i$.

(M-5) Then draw α circles and β circles on $\Sigma_i \setminus (z \cup w)$, such that the following hold.

(a) The α circles and β circles are transverse to each other and to ∂S_i.

(b) The α circles are pairwise disjoint and they span a half-dimensional subspace of $H_1(\Sigma_i)$; each component of $\Sigma_i \setminus \alpha$ contains a z marking and a w marking.

(c) The β circles are pairwise disjoint and they span a half-dimensional subspace of $H_1(\Sigma_i)$; each component of $\Sigma_i \setminus \beta$ contains a z marking and a w marking.

(d) Each component of $\Sigma_1 \setminus \alpha$ (respectively, $\Sigma_2 \setminus \beta$) has an oriented arc in $(-1)^i \partial S_i$ joining the w marking to the z marking.

(e) Exactly $(l_i + \delta_i - \chi(R_i))$ β (respectively, α) circles intersect S_1 (respectively, S_2).

(f) There are exactly $(n-1)$ α circles lying entirely inside the 2-sphere S^2, and they encircle the edges A_3A_4, A_5A_6, …, $A_{2n-1}A_{2n}$. There are exactly $(n-1)$ β circles lying entirely inside the 2-sphere S^2, and they encircle the intervals A_4A_5, A_6A_7, …, $A_{2n}A_1$. Moreover, the consecutive α and β circles intersect each other at exactly two points.

(g) Other than the above circles, there are no β (respectively, α) circle of Σ_1 (respectively, Σ_2) that intersects S^2. There could be some α (respectively, β) arcs of Σ_1 (respectively, Σ_2) that intersect S^2; in that case, their intersection with S^2 lies entirely inside $S_i \cap S^2$; and we can also ensure that there are at most $(n-1)$ of such α (respectively, β) arcs.

(M-6) We then do finger moves on the β (respectively, α) circles on Σ_1 (respectively, Σ_2) to convert this to a Heegaard diagram $\mathcal{H}_1$ (respectively, $\mathcal{H}_2$) adapted to the Seifert surface R_1 (respectively, R_2). These final diagrams, in the case when $n = 2$, are shown in Figure 2.4. In the case when $n = 3$,

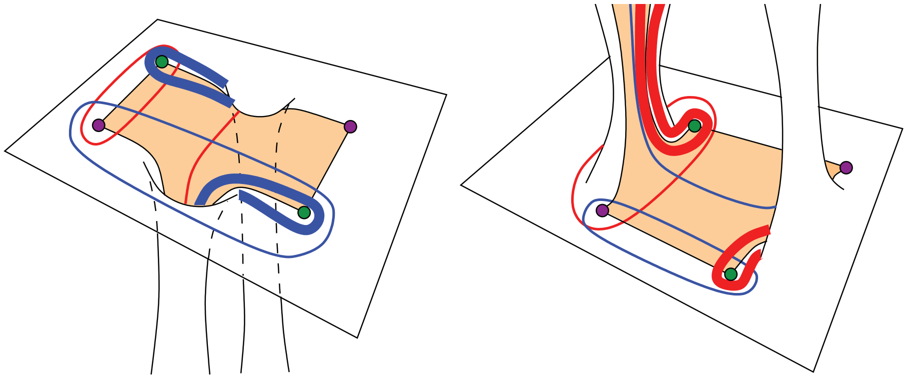

Figure 2.4. The Heegaard diagrams $\mathcal{H}_1$ and $\mathcal{H}_2$. We continue to represent w and z markings by magenta and green dots, respectively. Once again, the thin lines are curves, and the thick lines are train tracks, representing some (possibly zero) curves running in parallel.

the diagrams are also shown in the first two figures of the top row of Figure 4.1 (where X denotes a handle going down into B_1 and O denotes a handle coming up into B_2).

(M-7) The first two figures in the third row of Figure 4.1 represent slightly modified Heegaard diagrams $\mathcal{H}_i''$ that are obtained from $\mathcal{H}_i$ by deleting the z-markings, modifying the surface S_i, and performing small isotopies to reduce the number of intersections between α and β circles. We will assume that we have already performed some isotopies on the α and β circles on $\mathcal{H}_i$ away from S^2 so as to ensure that these modified diagrams $\mathcal{H}_i''$, and hence $\mathcal{H}_i$ itself, is already admissible.

We can now "combine" the Heegaard diagram $\mathcal{H}_1$ adapted to R_1 and $\mathcal{H}_2$ adapted to R_2 to form a Heegaard diagram $\mathcal{H}_1 * \mathcal{H}_2$ adapted to $R_1 * R_2$. Recall that in $\mathcal{H}_1$, the α-handlebody $U_{\alpha,1}$ is obtained by tunneling out a few one-handles from $\overline{B_1}$, and the β-handlebody $U_{\beta,1}$ is obtained by attaching those corresponding one-handles to $\overline{B_2}$. Similarly, in $\mathcal{H}_2$, the α-handlebody $U_{\alpha,2}$ is obtained by attaching a few one-handles to $\overline{B_1}$, and the β-handlebody $U_{\beta,2}$ is obtained by tunneling out those corresponding one-handles from $\overline{B_2}$. In the "combined" Heegaard diagram $\mathcal{H}_1 * \mathcal{H}_2$, the α-handlebody $U_{\alpha,1} * U_{\alpha,2}$ is obtained from $\overline{B_1}$ by tunneling out all the one-handles that were tunneled out in $U_{\alpha,1}$ and by attaching all the one-handles that were attached in $U_{\alpha,2}$, and the β-handlebody $U_{\beta,1} * U_{\beta,2}$ is the closure of its complement. The Heegaard surface $\Sigma_1 * \Sigma_2$ is the oriented boundary of $U_{\alpha,1} * U_{\alpha,2}$. There is a surface $S_1 * S_2 \subset \Sigma_1 * \Sigma_2$, isotopic to $R_1 * R_2$, which is obtained from $S_1 \subset \Sigma_1$ and $S_2 \subset \Sigma_2$. The w and z basepoints, and the α and β circles on $\Sigma_1 * \Sigma_2$ are induced

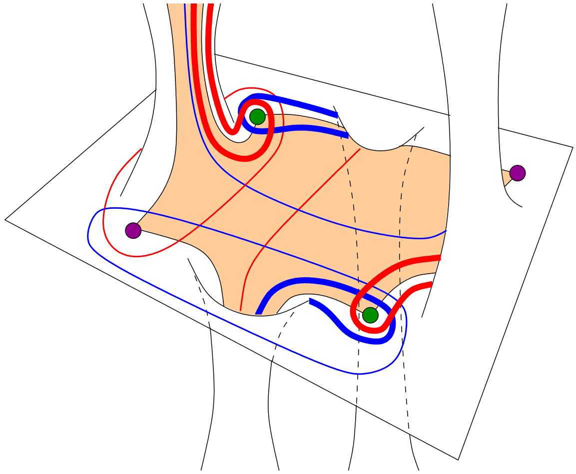

Figure 2.5. The Heegaard diagram $\mathcal{H}_1 * \mathcal{H}_2$. This diagram is obtained by combining the Heegaard diagrams $\mathcal{H}_1$ and $\mathcal{H}_2$ from Figure 2.4

from the corresponding objects in Σ_1 and Σ_2. The Heegaard diagram $\mathcal{H}_1 * \mathcal{H}_2$, in the case when $n = 2$, looks like Figure 2.5, and in the case $n = 3$, looks like the third figure in the top row of Figure 4.1. Since the modified diagrams $\mathcal{H}_1''$ and $\mathcal{H}_2''$ are admissible, it follows that the corresponding modified diagram $(\mathcal{H}_1 * \mathcal{H}_2)''$ (third figure in the third row of Figure 4.1), and hence $\mathcal{H}_1 * \mathcal{H}_2$ itself, is also admissible.

3. Certain local isotopies

Let $\mathcal{H}_{\alpha\beta} = (\Sigma_{(g)}, \alpha^{(g+k-1)}, \beta^{(g+k-1)}, w^{(k)})$ be a Heegaard diagram for S^3, which possibly is non-admissible, and $S \subset \Sigma$ be an open subsurface. Let $\mathcal{A}_{\mathcal{H}_{\alpha\beta},S} \subseteq \mathcal{G}_{\mathcal{H}_{\alpha\beta}}$ be the set of all the generators, none of whose coordinates lie inside S, and let $\mathcal{B}_{\mathcal{H}_{\alpha\beta},S} = \mathcal{G}_{\mathcal{H}_{\alpha\beta}} \setminus \mathcal{A}_{\mathcal{H}_{\alpha\beta},S}$ denote the rest of the generators. Let us assume that S contains a disk D that looks like the first part of Figure 3.1 (with the train track convention): there are b β arcs, all parallel to each other, with $b \geq 1$; there are $a_1 + 1 + a_2$ α arcs, all parallel to each other, with $a_1, a_2 \geq 0$, such that a_2 of them are disjoint from the β arcs, and each of the $a_1 + 1$ others, intersect each of the b β arcs in exactly two points; there is a w marking, such that the oriented boundary of the component of $D \setminus (\alpha \cup \beta)$ containing the w marking, is an α arc followed by a β arc followed by an arc in ∂D. Note that these b β arcs need not belong to b different β circles, and these $a_1 + 1 + a_2$ α arcs need not belong to $a_1 + 1 + a_2$ different α circles.

Let $\mathcal{H}_{\gamma\beta} = (\Sigma, \gamma, \beta, w)$ be the Heegaard diagram (also possibly non-admissible) obtained from $\mathcal{H}$ after the local isotopy as shown in Figure 3.1. The surface Σ, the

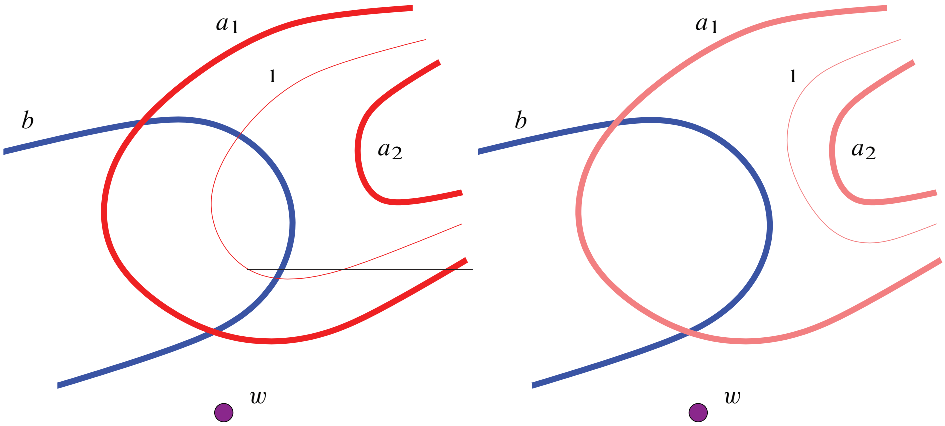

Figure 3.1. The disk D in the Heegaard diagrams $\mathcal{H}_{\alpha\beta}$ and $\mathcal{H}_{\gamma\beta}$. The α, β, and γ arcs are represented by red, blue, and pink train tracks, respectively, with thin lines denoting curves. The number of arcs in each train track is also shown.

β circles, the w markings, and the subsurface S are unchanged. The α circles are replaced by the γ circles, which for the most part, are small perturbations of the corresponding α circles, except for one of the arcs in the disk D. There are $a_1 + 1 + a_2$ γ arcs in $D \subset S \subset \Sigma$ in $\mathcal{H}_{\gamma\beta}$, of which $1 + a_2$ of them are disjoint from the β arcs, and each of the remaining a_1 of them intersect each of the b β arcs in exactly two points. This is shown in the second part of Figure 3.1, with the γ train tracks and arcs being denoted by thick and thin pink lines respectively. Once again, let $\mathcal{A}_{\mathcal{H}_{\gamma\beta},S} \subset \mathcal{G}_{\mathcal{H}_{\gamma\beta}}$ be the set of all the generators, none of whose coordinates lie inside S, and let

$$\mathcal{B}_{\mathcal{H}_{\gamma\beta},S} = \mathcal{G}_{\mathcal{H}_{\gamma\beta}} \setminus \mathcal{A}_{\mathcal{H}_{\gamma\beta},S}$$

denote the rest of the generators. There is an obvious bijection $\mathcal{A}_{\mathcal{H}_{\alpha\beta},S} \xrightarrow{\cong} \mathcal{A}_{\mathcal{H}_{\gamma\beta},S}$, and we will always implicitly identify them by this bijection; there is an obvious injection $\mathcal{B}_{\mathcal{H}_{\gamma\beta},S} \hookrightarrow \mathcal{B}_{\mathcal{H}_{\alpha\beta},S}$, and we will always implicitly treat $\mathcal{B}_{\mathcal{H}_{\gamma\beta},S}$ as a subset of $\mathcal{B}_{\mathcal{H}_{\alpha\beta},S}$ by this injection.

Proposition 3.1. *If there are no empty positive domains from $\mathcal{A}_{\mathcal{H}_{\alpha\beta},S}$ to $\mathcal{B}_{\mathcal{H}_{\alpha\beta},S}$, then there are no empty positive domains from $\mathcal{A}_{\mathcal{H}_{\gamma\beta},S}$ to $\mathcal{B}_{\mathcal{H}_{\gamma\beta},S}$.*

Proof. We will prove the contrapositive of the statement. The basic idea is that any positive domain from $\mathcal{A}_{\mathcal{H}_{\gamma\beta},S}$ to $\mathcal{B}_{\mathcal{H}_{\gamma\beta},S}$ induces a corresponding positive domain in the original diagram, simply by tracing multiplicities through the reversal of the isotopy. To make this precise, let us assume that $D_1 \in \mathcal{D}_0(x, y)$ is a positive domain, from some generator $x \in \mathcal{A}_{\mathcal{H}_{\gamma\beta},S}$ to some generator $y \in \mathcal{B}_{\mathcal{H}_{\gamma\beta},S}$. Let $\bar{x} \in \mathcal{A}_{\mathcal{H}_{\alpha\beta},S}$ and $\bar{y} \in \mathcal{B}_{\mathcal{H}_{\alpha\beta},S}$ be the images of x and y under the bijection $\mathcal{A}_{\mathcal{H}_{\gamma\beta},S} \xrightarrow{\cong} \mathcal{A}_{\mathcal{H}_{\alpha\beta},S}$

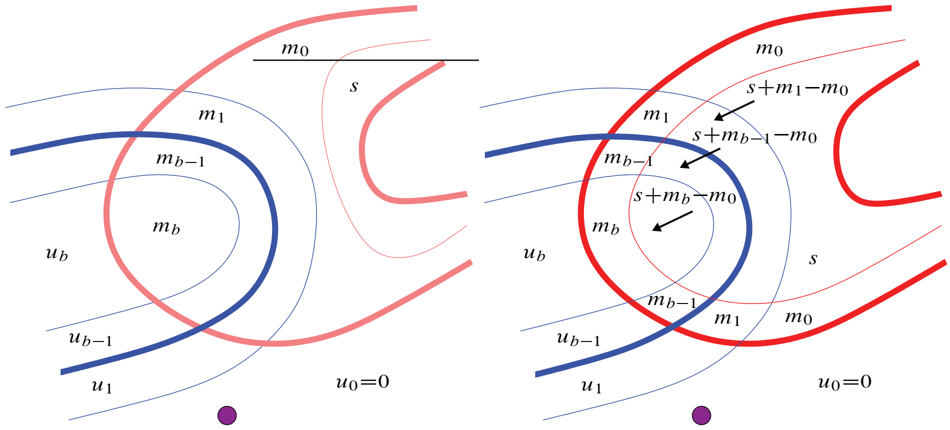

Figure 3.2. The local coefficients of D_1 and D_2 in $\mathcal{H}_{\gamma\beta}$ and $\mathcal{H}_{\alpha\beta}$. We prove that if D_1 is a positive domain, then so is D_2, which follows once we show that $s + m_i - m_0 \geq s + u_i$.

and the injection $\mathcal{B}_{\mathcal{H}_{\gamma\beta},\mathfrak{s}} \hookrightarrow \mathcal{B}_{\mathcal{H}_{\alpha\beta},\mathfrak{s}}$, respectively. The empty domain D_1 gives rise to another empty domain $D_2 \in \mathcal{D}_0(\bar{x}, \bar{y})$. The local coefficients of D_1 and D_2 are shown in Figure 3.2. We will simply show that D_2 is also a positive domain.

Towards this end, we will prove that none of the coefficients $m_1, \ldots, m_b$ are smaller than the coefficient m_0. We will prove this by showing that $u_i \leq m_i - m_0$, for all $0 \leq i \leq b$. Since each $u_i \geq 0$, this will complete the proof.

We will prove $u_i \leq m_i - m_0$ by an induction on i. Since, $u_0 = 0 = m_0 - m_0$, the base case is trivial. Assume by induction that the statement is true for i. Before we prove the statement for $i + 1$, let us make one small observation about the domain D_1.

Since $\partial(\partial D_1 \cap \beta) = x - y$, and since none of the coordinates of x lie in the disk D, we therefore have that $\partial(\partial D_1 \cap \beta)$, viewed as a 0-chain, does not contain any point with positive sign in the local neighborhood D. Let τ be an oriented arc, which is a subspace of a β circle, and is supported entirely inside D. Let the coefficient of $\partial D_1 \cap \beta$ near the beginning of τ be $c > 0$. The observation that $\partial(\partial D_1 \cap \beta)$ does not contain any positively signed point in D, implies that the coefficient of $\partial D_1 \cap \beta$ near the end of τ is greater than or equal to c. We summarize this observation by the statement that "$\partial D_1 \cap \beta$ does not stop inside D."

Now, we are all set to prove the induction statement for $i + 1$. In the Heegaard diagram $\mathcal{H}_{\gamma\beta}$, let β_1 be the β circle that separates the elementary region with coefficient m_{i+1} from the elementary region with coefficient m_i, and let τ be an oriented subarc of β_1, running from the elementary region with coefficient m_i to the elementary region with coefficient u_i. Therefore, the signed coefficients of $\partial D_1 \cap \beta$ near the beginning and the end of τ are $m_i - m_{i+1}$ and $u_i - u_{i+1}$ respectively, as shown in

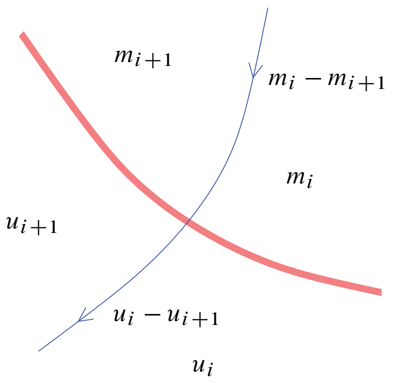

Figure 3.3. The induction step. Assuming $u_i \leq m_i - m_0$, we prove $u_{i+1} \leq m_{i+1} - m_0$ by showing $u_{i+1} - u_i \leq m_{i+1} - m_i$. The coefficients of D_1 and the coefficients of $\partial D_1 \cap \beta$ are shown.

Figure 3.3. (These coefficients could be negative, but that does not affect the proof.) In light of the observation above that $\partial D_1 \cap \beta$ does not stop inside D, it follows that coefficient of $\partial D_1 \cap \beta$ near the end of τ is greater than or equal to that at the end:

$$m_i - m_{i+1} \leq u_i - u_{i+1}.$$

Subtracting m_0 from both sides of the inequality, and rearranging, we have

$$u_{i+1} + m_i - m_0 - u_i \leq m_{i+1} - m_0$$

But the inductive hypothesis is that $0 \leq m_i - m_0 - u_i$, hence $u_{i+1} \leq m_{i+1} - m_0$, as desired. ∎

Now, we prove a similar statement for triangular domains. Let $\mathcal{H}_{\alpha\beta\gamma} = (\Sigma, \alpha, \beta, \gamma, w)$ be the triple Heegaard diagram, obtained by combining the above two diagrams; it is also possibly non-admissible. We assume that γ_i is a small translate of α_i, intersecting it transversely in exactly two points, so that γ_i is disjoint from α_j for $i \neq j$. Let α_1 be the α circle that is changed to the γ circle γ_1 in Figure 3.4. Therefore, a neighborhood N_i of $\alpha_i \cup \gamma_i$ for $i \neq 1$ looks like the first part of Figure 3.5, with none of the two intersection points in $\alpha_i \cap \gamma_i$ lying in the neighborhood D. A neighborhood N_1 of $\alpha_1 \cup \gamma_1$ looks like the second part of Figure 3.5, with both the intersection points in $\alpha_1 \cap \gamma_1$ lying in the neighborhood D. The coordinates of the top generator θ are shown.

Proposition 3.2. *If there are no empty positive domains from $\mathcal{A}_{\mathcal{H}_{\alpha\beta},S}$ to $\mathcal{B}_{\mathcal{H}_{\alpha\beta},S}$, then there are no empty positive triangular domains from $\mathcal{A}_{\mathcal{H}_{\alpha\beta},S}$ to $\mathcal{B}_{\mathcal{H}_{\gamma\beta},S}$.*

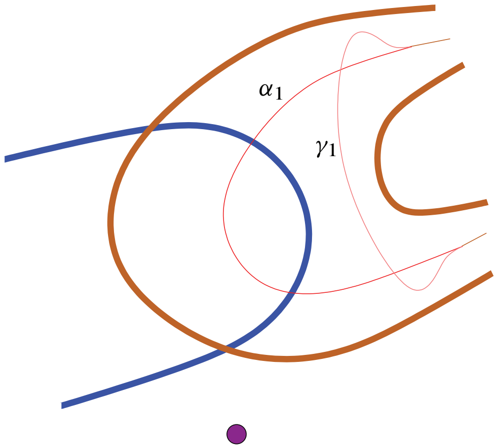

Figure 3.4. The Heegaard diagram $\mathcal{H}_{\alpha\beta\gamma}$ in the neighborhood D. As before, α, β, γ are red, blue, and pink, respectively. A thin brown curve denotes a train track which is pair of parallel α and γ curves, and a thick brown curve is a train track of such train tracks.

Proof. Let $D_1 \in \mathcal{T}_0(x, y)$ be a positive triangular domain, for some $x \in \mathcal{A}_{\mathcal{H}_{\alpha\beta},S}$ and $y \in \mathcal{B}_{\mathcal{H}_{\gamma\beta},S}$. Let $\bar{y} \in \mathcal{B}_{\mathcal{H}_{\alpha\beta},S}$ be the image of y under the injection $\mathcal{B}_{\mathcal{H}_{\gamma\beta},S} \hookrightarrow \mathcal{B}_{\mathcal{H}_{\alpha\beta},S}$. It is easy to see that there is a unique empty triangular domain $D_2 \in \mathcal{T}_0(\bar{y}, y)$, whose non-zero coefficients are supported inside the neighborhoods N_i, such that $\partial D_2 \cap \gamma = \partial D_1 \cap \gamma$; this domain D_2 typically will have both positive and negative coefficients. Then, the 2-chain $D_3 = D_1 - D_2$ is a domain in $\mathcal{D}_0(x, \bar{y})$. We will show that D_3 is also a positive domain, establishing the contrapositive of the given statement.

The coefficients of D_2 are zero outside $\bigcup_i N_i$, and the neighborhoods N_i for $i \neq 1$ can be considered as special cases of the neighborhood N_1. Therefore, we only need to concentrate on the coefficients of D_3 in N_1. Figure 3.6 shows the coefficients of D_1, $\partial D_1 \cap \gamma_1$ and D_3 in this neighborhood. The coordinates of θ and y on γ_1 are shown. The coefficient of $\partial D_1 \cap \gamma_1$ is either r or $r + 1$ (which need not be positive), as shown.

Since D_1 is a positive domain, and since the region with coefficient q_ℓ in D_1 has γ_1 on its boundary with coefficient $r + 1$, we must have $q_\ell \geq r + 1$ for all $1 \leq \ell \leq d$. Similarly, we must have $p_\ell \geq r$ for all $1 \leq \ell \leq c$ and $m_0 \geq -r$. Therefore, in order to show that D_3 is also a positive domain, we only need to show that each of the coefficients $m_1, \ldots, m_b$ are greater than or equal to $-r$. However, exactly as in the proof of Proposition 3.1, using the fact that x has no coordinates inside the disk D, we can show that none of the coefficients $m_1, \ldots, m_b$ are smaller than m_0, and this completes the proof. ∎

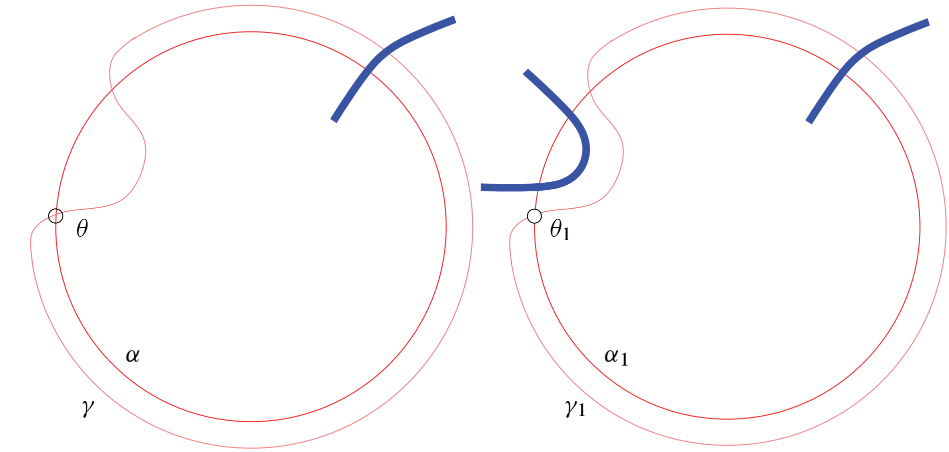

Figure 3.5. Neighborhoods N_i of $\alpha_i \cup \gamma_i$. For $i \neq 1$ (left), the small bigon region is disjoint from D, while for $i = 1$ (right), the small bigon region is contained inside D. The coordinates of the top generator θ are shown by white dots.

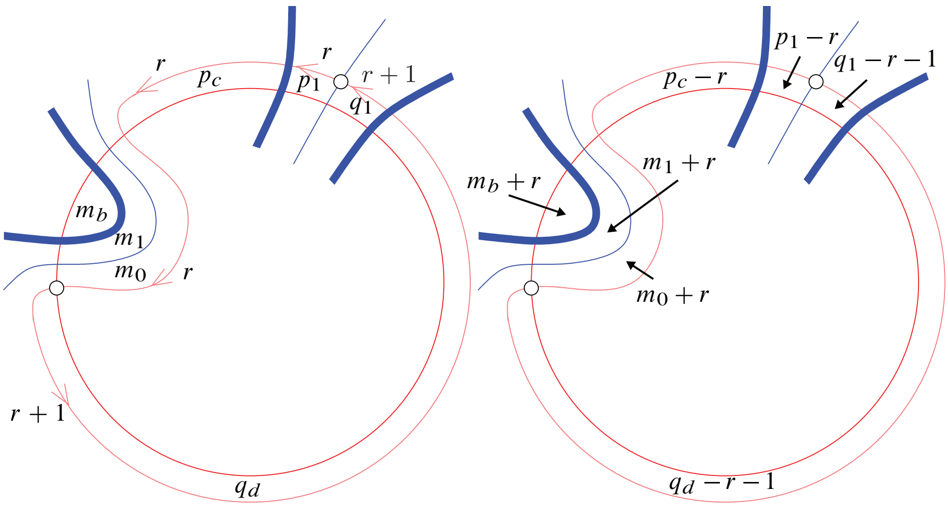

Figure 3.6. Coefficients of D_1 (left) and D_3 (right) in the neighborhood N_1 of $\alpha_1 \cup \gamma_1$. The coordinates of θ and y are shown by white dots. The coefficients of $\partial D_1 \cap \gamma_1$ are also shown on the left.

Let us henceforth assume that the Heegaard diagram $\mathcal{H}_{\gamma\beta}$ is admissible. Then $\mathcal{H}_{\alpha\beta}$ and $\mathcal{H}_{\alpha\beta\gamma}$ are also admissible, and in that case, $\widetilde{CF}_{\mathcal{H}_{\alpha\beta}}$ and $\widetilde{CF}_{\mathcal{H}_{\gamma\beta}}$ are the chain complexes, freely generated over $\mathbb{F}_2$, by $\mathcal{G}_{\mathcal{H}_{\alpha\beta}}$ and $\mathcal{G}_{\mathcal{H}_{\gamma\beta}}$, respectively. Let $\widetilde{SF}_{\mathcal{H}_{\alpha\beta},S}$ and $\widetilde{SF}_{\mathcal{H}_{\gamma\beta},S}$ be the $\mathbb{F}_2$-submodules, freely generated by $\mathcal{A}_{\mathcal{H}_{\alpha\beta},S}$ and $\mathcal{A}_{\mathcal{H}_{\gamma\beta},S}$, respectively.

Theorem 3.3. *Assume that there are no empty positive domains from $\mathcal{A}_{\mathcal{H}_{\alpha\beta},S}$ to $\mathcal{B}_{\mathcal{H}_{\alpha\beta},S}$. Then $\widetilde{SF}_{\mathcal{H}_{\alpha\beta},S}$ is a subcomplex of $\widetilde{CF}_{\mathcal{H}_{\alpha\beta}}$, $\widetilde{SF}_{\mathcal{H}_{\gamma\beta},S}$ is a subcomplex of $\widetilde{CF}_{\mathcal{H}_{\gamma\beta}}$, and the chain map from $\widetilde{CF}_{\mathcal{H}_{\alpha\beta}}$ to $\widetilde{CF}_{\mathcal{H}_{\gamma\beta}}$ induces a chain map from $\widetilde{SF}_{\mathcal{H}_{\alpha\beta},S}$ to $\widetilde{SF}_{\mathcal{H}_{\gamma\beta},S}$. Furthermore, the chain maps $\widetilde{CF}_{\mathcal{H}_{\alpha\beta}} \to \widetilde{CF}_{\mathcal{H}_{\gamma\beta}}$ and $\widetilde{SF}_{\mathcal{H}_{\alpha\beta},S} \to \widetilde{SF}_{\mathcal{H}_{\gamma\beta},S}$ are quasi-isomorphisms.*

Proof. Proposition 3.1 implies that there are no empty positive domains from $\mathcal{A}_{\mathcal{H}_{\gamma\beta},S}$ to $\mathcal{B}_{\mathcal{H}_{\gamma\beta},S}$, and Proposition 3.2 implies that there are no empty positive triangular domains from $\mathcal{A}_{\mathcal{H}_{\alpha\beta},S}$ to $\mathcal{B}_{\mathcal{H}_{\gamma\beta},S}$. Since the non-zero terms in the boundary maps on $\widetilde{CF}_{\mathcal{H}_{\alpha\beta}}$ and $\widetilde{CF}_{\mathcal{H}_{\gamma\beta}}$ come only from empty positive domains, and the non-zero terms in the chain map from $\widetilde{CF}_{\mathcal{H}_{\alpha\beta}}$ to $\widetilde{CF}_{\mathcal{H}_{\gamma\beta}}$ come only from empty positive triangular domains, $\widetilde{SF}_{\mathcal{H}_{\alpha\beta},S} \hookrightarrow \widetilde{CF}_{\mathcal{H}_{\alpha\beta}}$ is a subcomplex, $\widetilde{SF}_{\mathcal{H}_{\gamma\beta},S} \hookrightarrow \widetilde{CF}_{\mathcal{H}_{\gamma\beta}}$ is a subcomplex, and the chain map $\widetilde{CF}_{\mathcal{H}_{\alpha\beta}} \to \widetilde{CF}_{\mathcal{H}_{\gamma\beta}}$ induces a chain map $\widetilde{SF}_{\mathcal{H}_{\alpha\beta},S} \to \widetilde{SF}_{\mathcal{H}_{\gamma\beta},S}$, resulting in the following commuting square:

$$\begin{array}{ccc} \widetilde{SF}_{\mathcal{H}_{\alpha\beta},S} & \hookrightarrow & \widetilde{CF}_{\mathcal{H}_{\alpha\beta}} \\ \downarrow & & \downarrow \\ \widetilde{SF}_{\mathcal{H}_{\gamma\beta},S} & \hookrightarrow & \widetilde{CF}_{\mathcal{H}_{\gamma\beta}} \end{array}$$

We will now show that the vertical arrows induce isomorphisms on homology. A 2-*cochain* on a Heegaard diagram or a triple Heegaard diagram is a map which assigns real numbers to the elementary regions; a *non-negative* 2-*cochain* is a 2-cochain which only assigns non-negative numbers; and a *positive* 2-*cochain* is a 2-cochain which only assigns positive numbers. Since $\mathcal{H}_{\gamma\beta}$ is admissible, by repeating the proof of [27, Lemma 4.12], there exists a positive 2-cochain C_0 on $\mathcal{H}_{\gamma\beta}$, which evaluates to zero on all empty periodic domains in $\mathcal{H}_{\gamma\beta}$. Indeed, while we use the notion of admissibility for Heegaard diagrams arising from Morse functions with additional index 0 and 3 critical points [29, Definition 3.5], the proof of [27, Lemma 4.12] carries through verbatim.

A cochain in $\mathcal{H}_{\alpha\beta\gamma}$ induces cochains in $\mathcal{H}_{\alpha\beta}$ and $\mathcal{H}_{\gamma\beta}$, by forgetting the γ circles and the α circles, respectively, as well as the coefficients of the cochain on the thin elementary regions that lie entirely inside the neighborhoods N_i. We will now construct a non-negative cochain C on $\mathcal{H}_{\alpha\beta\gamma}$, such that C assigns zero precisely to the elementary regions that lie entirely in the neighborhoods N_i; and C induces the positive cochain C_0 in $\mathcal{H}_{\gamma\beta}$. Since the empty periodic domains in $\mathcal{H}_{\alpha\beta\gamma}$ are generated by the empty periodic domains in $\mathcal{H}_{\gamma\beta}$ and the periodic domains that are supported in $\bigcup_i N_i$, this would imply that C evaluates to zero on any empty periodic domain in

$\mathcal{H}_{\alpha\beta\gamma}$. The way to construct C is fairly straightforward. Let R be an elementary region in $\mathcal{H}_{\gamma\beta}$, and let r be the assignment of C_0 on R. The region R might get cut up into several elementary regions $R_1, \ldots, R_n$ in $\mathcal{H}_{\alpha\beta\gamma}$, and some of them might lie entirely in the neighborhoods N_i, but at least one of them does not. Choose non-negative real numbers $r_1, \ldots, r_n$, such that, $\sum_i r_i = r$ and $r_i = 0$ if and only if R_i lies entirely in $\bigcup_i N_i$. Then assign the number r_i to the elementary region R_i in the 2-cochain C.

This non-negative 2-cochain C gives rise to filtrations on the mapping cones $\widetilde{SF}_{\mathcal{H}_{\alpha\beta},S} \to \widetilde{SF}_{\mathcal{H}_{\gamma\beta},S}$ and $\widetilde{CF}_{\mathcal{H}_{\alpha\beta}} \to \widetilde{CF}_{\mathcal{H}_{\gamma\beta}}$, as follows: given any two generators $x, y \in \mathcal{G}_{\mathcal{H}_{\alpha\beta}} \cup \mathcal{G}_{\mathcal{H}_{\gamma\beta}}$, the relative filtration grading between them is $\langle C, D\rangle$, for any D in $\mathcal{D}_0(x, y)$ or $\mathcal{T}_0(x, y)$ as the case may be. On the associated graded level, we only count domains or triangular domains that lie entirely inside these neighborhoods N_i, and then it is fairly straightforward to check that the associated graded maps on the associated graded objects are isomorphisms, and therefore, the original chain maps must have been quasi-isomorphisms as well. ■

4. Main theorems

Proof of Theorem 1.1. Following the notations from Section 2.4, let $\mathcal{H}_1$, $\mathcal{H}_2$ and $\mathcal{H}_1 * \mathcal{H}_2$, as shown in Figures 2.4 and 2.5, be the Heegaard diagrams adapted to Seifert surfaces R_1, R_2 and $R_1 * R_2$ for the links L_1, L_2 and $L = L_1 * L_2$, respectively. The corresponding Heegaard surfaces contain embedded subsurfaces S_1, S_2 and $S_1 * S_2$, which represent R_1, R_2 and $R_1 * R_2$, respectively. Furthermore, $\mathcal{H}_1$ has $(l_1 + \delta_1)$ w-markings, $\mathcal{H}_2$ has $(l_2 + \delta_2)$ w-markings, $\mathcal{H}_1 * \mathcal{H}_2$ has $(l + \delta)$ w-markings.

Thanks to Corollary 2.9, we only need to produce an isomorphism of graded chain complexes

$$\begin{aligned}
&\mathcal{F}_{\mathcal{H}_1 * \mathcal{H}_2}\Big(-\frac{1}{2}(l + 2\delta - \chi(R_1 * R_2))\Big)[l + \delta - 1] \\
&\quad\cong \mathcal{F}_{\mathcal{H}_1}\Big(-\frac{1}{2}(l_1 + 2\delta_1 - \chi(R_1))\Big)[l_1 + \delta_1 - 1] \\
&\qquad\otimes \mathcal{F}_{\mathcal{H}_2}\Big(-\frac{1}{2}(l_2 + 2\delta_2 - \chi(R_2))\Big)[l_2 + \delta_2 - 1],
\end{aligned}$$

or in terms of the notation from Section 3, since $(l + \delta - n) = (l_1 + \delta_1 - n) + (l_2 + \delta_2 - n)$,

$$\widetilde{SF}_{\mathcal{H}_1 * \mathcal{H}_2, S_1 * S_2}[n - 1] \cong \widetilde{SF}_{\mathcal{H}_1, S_1}[n - 1] \otimes \widetilde{SF}_{\mathcal{H}_2, S_2}[n - 1]. \tag{4.1}$$

Let $(\mathcal{H}, S)$ denote any of $(\mathcal{H}_1, S_1)$, $(\mathcal{H}_2, S_2)$, or $(\mathcal{H}_1 * \mathcal{H}_2, S_1 * S_2)$, as shown in the first row of Figure 4.1. The sphere S^2 of the Murasugi sum is represented by the squares on the page, with L_1 lying below the page and L_2 lying above. Let Σ be

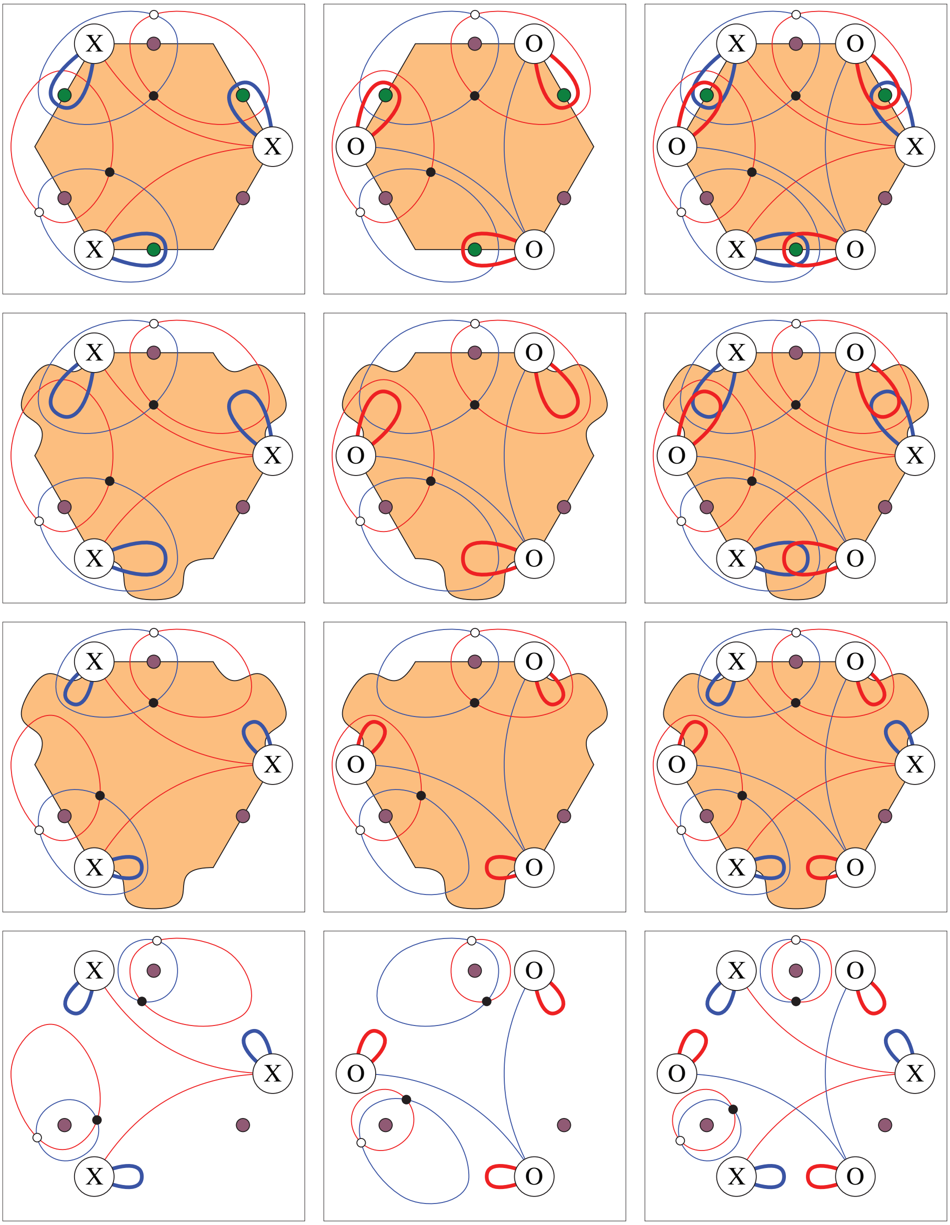

Figure 4.1. The Heegaard diagrams appearing in the proof of Theorems 1.1 and 1.2. The left, middle, right columns represent diagrams obtained from $\mathcal{H}_1$, $\mathcal{H}_2$, $\mathcal{H}_1 * \mathcal{H}_2$, respectively; the consecutive rows represent the diagrams $\mathcal{H}$, $\mathcal{H}'$, $\mathcal{H}''$, and $\mathcal{H}'''$; X and O denote handles going down (into the page) and up (towards the reader), respectively.

the Heegaard surface and let Σ^1 (respectively, Σ^2) be the portion of Σ that lies inside (respectively, outside) the sphere S^2.

Let $\mathcal{H}'$ be the Heegaard diagrams for S^3 obtained from $\mathcal{H}$ by forgetting the z markings, and let S' be the open subsurface of the Heegaard surface of $\mathcal{H}$, obtained by slightly modifying S in a neighborhood of the $2n$-gon $A_1 A_2 \dots A_{2n}$ so as to include all the intersections between α and β circles near the erstwhile z-markings. These modified diagrams $(\mathcal{H}', S')$ are shown in the second row of Figure 4.1.

Since we have not changed the underlying Heegaard diagrams, clearly, $\widetilde{CF}_{\mathcal{H}'} = \widetilde{CF}_{\mathcal{H}}$. Next we claim that any generator $x \in \mathcal{G}_{\mathcal{H}}$ that does not have any coordinate in S cannot have any coordinate in S' either. This is a simple counting argument. Indeed, let us say $\mathcal{H}_i$ has total of n_i α-circles and n_i β-circles; of them, exactly $(n-1)$ α-circles and $(n-1)$ β-circles lie entirely inside the S^2. Then $\mathcal{H}_1 * \mathcal{H}_2$ has a total of (n_1+n_2-n+1) α-circles and (n_1+n_2-n+1) β-circles, again with exactly $(n-1)$ α-circles and $(n-1)$ β-circles lying entirely inside the S^2. For $\mathcal{H} \neq \mathcal{H}_2$, we see that (n_1-n+1) α circles of $\mathcal{H}$ lie entirely within $\Sigma^1 \cup S$, and so x must have at least (n_1-n+1) coordinates in Σ^1 (as it avoids the surface S, by assumption). Similarly, for $\mathcal{H} \neq \mathcal{H}_1$, we see that (n_2-n+1) β circles of $\mathcal{H}$ lie entirely within $\Sigma^2 \cup S$, and so x must have at least (n_2-n+1) coordinates in Σ^2. Therefore, in all cases, x has at most $(n-1)$ coordinates in the sphere S^2. It follows that, in fact, x must have exactly $(n-1)$ coordinates in the sphere, occupied by the $(n-1)$ α and β circles that lie entirely therein. Specifically, they must be the white dots as shown in the first row of Figure 4.1. Therefore, we get that $\widetilde{SF}_{\mathcal{H}',S'} = \widetilde{SF}_{\mathcal{H},S}$. Moreover, since there are no positive domains from generators of $\widetilde{SF}_{\mathcal{H},S}$ to the other generators of $\widetilde{CF}_{\mathcal{H}}$ due to Alexander grading, there are no positive domains from the generators of $\widetilde{SF}_{\mathcal{H}',S'}$ to the other generators of $\widetilde{CF}_{\mathcal{H}'}$ as well, and we have the following identification of subcomplexes:

$$\begin{array}{ccc} \widetilde{SF}_{\mathcal{H},S} & \hookrightarrow & \widetilde{CF}_{\mathcal{H}} \\ \parallel & & \parallel \\ \widetilde{SF}_{\mathcal{H}',S'} & \hookrightarrow & \widetilde{CF}_{\mathcal{H}'} \end{array} \tag{4.2}$$

As in Section 3, we perform local isotopies to separate the α and β curves in the neighborhood of the erstwhile z-markings so that we obtain the Heegaard diagrams in the third row of Figure 4.1, which we denote by $(\mathcal{H}'', S')$. The aforementioned isotopies are supported inside S', and there are no domains from the generators of $\widetilde{SF}_{\mathcal{H}',S'}$ to the other generators of $\widetilde{CF}_{\mathcal{H}'}$. Recalling that the Heegaard diagrams were constructed to ensure that $\mathcal{H}''$ is admissible (see (M-7)), we see that the hypotheses of Theorem 3.3 are satisfied, and therefore, we obtain a quasi-isomorphism between the following two-step filtered complexes:

$$\begin{array}{ccc} \widetilde{SF}_{\mathcal{H}',S'} & \hookrightarrow & \widetilde{CF}_{\mathcal{H}'} \\ \text{q.i.}\downarrow & & \downarrow\text{q.i.} \\ \widetilde{SF}_{\mathcal{H}'',S'} & \hookrightarrow & \widetilde{CF}_{\mathcal{H}''} \end{array} \tag{4.3}$$

Next, we claim that for any generator x of $\widetilde{CF}_{\mathcal{H}''}$, all its coordinates in S^2 must be the white or black dots from the third row of Figure 4.1. It is once again a counting argument, but with the roles of α and β reversed. For $\mathcal{H}'' \neq \mathcal{H}_2''$, we see that $(n_1 - n + 1)$ β circles of $\mathcal{H}''$ have no intersections with α circles in S^2, so x must have at least $(n_1 - n + 1)$ coordinates in Σ^1. Similarly, for $\mathcal{H}'' \neq \mathcal{H}_1''$, we see that $(n_2 - n + 1)$ α circles of $\mathcal{H}''$ have no intersections with β circles in S^2, so x must have at least $(n_2 - n + 1)$ coordinates in Σ^2. In all cases, x has at most $(n-1)$ coordinates in the sphere S^2, and therefore, they must be occupied by the $(n-1)$ α and β circles that lie entirely in S^2; moreover, they must be the white or black dots as shown in the third row of Figure 4.1.

After numbering the α circles that lie entirely in S^2 arbitrarily (but consistently across Heegaard diagrams) from 1 to $n-1$, each generator x can be represented as a pair $(\vec{a}, x^o)$, where $\vec{a} = (a_1, \dots, a_{n-1}) \in \{0,1\}^{n-1}$ with $a_i = 0$ if and only if α_i contains the white dot, and x^o denotes the coordinates of x that lie outside S^2. Consider the usual partial order on $\{0,1\}^{n-1}$ with $\vec{a} \leq \vec{b}$ if $a_i \leq b_i$ for all i, and the usual L^1-norm on $\{0,1\}^{n-1}$ given by $|\vec{a}| = \sum_i a_i$. Since empty positive domains are not allowed to pass through the w markings, we see that if $D \in \mathcal{D}_0((\vec{a}, x^o), (\vec{b}, y^o))$ is an empty positive domain, then $\vec{b} \leq \vec{a}$. Let $\widetilde{CF}^W_{\mathcal{H}''}$ denote the subcomplex of $\widetilde{CF}_{\mathcal{H}''}$ spanned by generators with $\vec{a} = 0$, that is, generators with only white dots. Then we have nested subcomplexes

$$\widetilde{SF}_{\mathcal{H}'',S'} \hookrightarrow \widetilde{CF}^W_{\mathcal{H}''} \hookrightarrow \widetilde{CF}_{\mathcal{H}''}.$$

For any generator x of $\widetilde{CF}_{(\mathcal{H}_1 * \mathcal{H}_2)''}$, let x^i be all its coordinates that lie in Σ^i. Then the map

$$(\vec{0}, x^1, x^2) \mapsto (\vec{0}, x^1) \otimes (\vec{0}, x^2)$$

produces the following identification between the following chain groups:

$$\begin{array}{ccc} \widetilde{SF}_{(\mathcal{H}_1 * \mathcal{H}_2)'',(S_1 * S_2)'} & \hookrightarrow & \widetilde{CF}^W_{(\mathcal{H}_1 * \mathcal{H}_2)''} \\ \cong\downarrow & & \downarrow\cong \\ \widetilde{SF}_{\mathcal{H}_1'',S_1'} \otimes \widetilde{SF}_{\mathcal{H}_2'',S_2'} & \hookrightarrow & \widetilde{CF}^W_{\mathcal{H}_1''} \otimes \widetilde{CF}^W_{\mathcal{H}_2''} \end{array} \tag{4.4}$$

Let us now prove that the vertical arrows are relative Maslov grading preserving chain maps—that is, the above identifications are identifications of chain complexes, up to a single absolute Maslov grading shift. Let $(\vec{0}, x^1, x^2)$ and $(\vec{0}, y^1, y^2)$ be two generators of $\widetilde{CF}^W_{(\mathcal{H}_1 * \mathcal{H}_2)''}$ and let $D \in \mathcal{D}((\vec{0}, x^1, x^2), (\vec{0}, y^1, y^2))$ be an empty positive domain in $(\mathcal{H}_1 * \mathcal{H}_2)''$ connecting them. Such a domain has to be disjoint from S^2. Indeed, the fact the domain has no corner points in S^2 forces it to restrict to a periodic domain therein, which the admissibility condition then ensures is the trivial domain with zero multiplicities. It follows that D splits as a disjoint union $D^1 \cup D^2$ of empty positive domains, with $D^i \in \mathcal{D}((\vec{0}, x^i), (\vec{0}, y^i))$ in $\mathcal{H}_i''$. Recall from Section 2.2 that D can only contribute to the differential if one of D^1 and D^2 is the trivial domain. Furthermore, since such domains avoid S^2, we may choose complex structures (and their perturbations) for the three Heegaard diagrams so that they agree on Σ^1 and Σ^2 (and their corresponding symmetric products); therefore, if D^1 (respectively, D^2) is the trivial domain, then the contribution of D will agree with the contribution of D^2 (respectively, D^1). This is an instance of the *localization principle* [32, Section 9.4], and it establishes that the vertical arrows are chain maps, and indeed chain isomorphisms. To see that the vertical arrows also respect the relative Maslov gradings, consider generators $(0, x^i)$, $(0, y^i)$ of $\widetilde{CF}^W_{\mathcal{H}_i''}$, and choose empty domains D^i in $\mathcal{H}_i''$ (not necessarily positive) connecting them. In $\mathcal{H}_1''$ (respectively, $\mathcal{H}_2''$) consider the $(n-1)$ α (respectively, β) circles that lie entirely inside S^2; each of them bounds a disk also entirely inside S^2, and each such disk is comprised of two bigon-shaped elementary regions—one containing a basepoint, and one without. By adding some number of copies of these disks to the domain D^i, we can get a domain E^i (not necessarily empty) connecting $(0, x^i)$ to $(0, y^i)$ in $\mathcal{H}_i''$, which has coefficient zero in the bigon region that does not contain the basepoint. Simply by adding the underlying 2-chains, these two domains E^1 and E^2 induce a domain E in $(\mathcal{H}_1 * \mathcal{H}_2)''$ connecting $(0, x^1, y^1)$ to $(0, x^2, y^2)$. It follows from Lipshitz' Maslov index formula [16] that $\mu(E) = \mu(E^1) + \mu(E^2)$, and it is immediate that $n_w(E) = n_w(E^1) + n_w(E^2)$. Consequently, the relative Maslov grading is preserved. Therefore, in order to finish the proof, we only need to calculate the absolute Maslov grading shift under the given isomorphism of relatively $\mathbb{Z}$-graded chain complexes. We will calculate this shift using the triangle maps associated to handleslides of the circles in S^2 over curves in the remainder of the diagram.

Towards this end, modify the Heegaard diagrams $\mathcal{H}''$ once more to get the Heegaard diagrams $\mathcal{H}'''$ of the fourth row of Figure 4.1. Namely, we slide the α circles inside S^2 off the attaching handles of Σ^2 (the ones marked O in Figure 4.1) and we slide the β circles inside S^2 off the attaching handles of Σ^1 (the ones marked X in Figure 4.1). There is an obvious identification between α circles, β circles, and generators $(\vec{a}, x^o)$ of $\mathcal{H}''$ and the corresponding objects of $\mathcal{H}'''$; let $\bar{\alpha}$, $\bar{\beta}$, and $(\vec{a}, \bar{x}^o)$ denote the corresponding objects in $\mathcal{H}'''$. Then each α circle only intersects the corresponding $\bar{\alpha}$ circle, and does so at two points. So, the Heegaard diagram $(\Sigma, \alpha, \beta, \bar{\alpha})$ is of the type as described in Section 2.3. The top generator θ has coordinates just next the white dots of $\mathcal{H}''$ and $\mathcal{H}'''$, and indeed, there is a small Maslov index zero triangular domain connecting $(\vec{0}, x^o)$ and $(\vec{0}, \bar{x}^o)$. Therefore, the Maslov grading of $(\vec{0}, x^o)$ is same as the Maslov grading of $(\vec{0}, \bar{x}^o)$. A similar argument, but with the roles of α and β reversed, proves that the Maslov grading is preserved under the handleslides of the β-circles as well.

Now, $\widetilde{CF}_{\mathcal{H}'''}$ decomposes into 2^{n-1} direct summands, one for each $\vec{a} \in \{0,1\}^{n-1}$. Moreover, the map $(0, x^o) \mapsto (\vec{a}, x^o)$ is an isomorphism between $\widetilde{CF}^W_{\mathcal{H}'''}[|\vec{a}|]$ and the summand corresponding to $\vec{a}$. Let $\mathcal{H}'''_d$ denote the Heegaard diagram destabilized $n-1$ times, obtained from $\mathcal{H}'''$ by removing the $(n-1)$ α and β circles that lie inside S^2, and the $(n-1)$ w-markings enclosed by them. Then, by Theorem 2.5,

$$\widetilde{CF}^W_{\mathcal{H}'''}[n-1] \cong \widetilde{CF}_{\mathcal{H}'''_d} \tag{4.5}$$

via the map $(\vec{0}, x^o) \mapsto x^o$.

Now, the map $(x^1, x^2) \mapsto x^1 \otimes x^2$ produces an identification of chain groups following a similar but simpler argument of equation 4.4:

$$\widetilde{CF}_{(\mathcal{H}_1 * \mathcal{H}_2)'''_d} \cong \widetilde{CF}_{(\mathcal{H}_1)'''_d} \otimes \widetilde{CF}_{(\mathcal{H}_2)'''_d}. \tag{4.6}$$

Moreover, this map is a relative Maslov grading preserving chain map, using a similar (but easier) localization principle argument to that above. However, $(\mathcal{H}_1)'''_d$, $(\mathcal{H}_2)'''_d$, and $(\mathcal{H}_1 * \mathcal{H}_2)'''_d$ are Heegaard diagrams for S^3 with $(l_1 + \delta_1 - n + 1)$, $(l_2 + \delta_2 - n + 1)$, and $(l + \delta - n + 1)$ basepoints, respectively; therefore, by Theorem 2.5 (and since $(l_1 + \delta_1 - n) + (l_2 + \delta_2 - n) = (l + \delta - n)$), either side of the equation has homology $\otimes^{l+\delta-n}(\mathbb{F}_2 \oplus \mathbb{F}_2[-1])$, so the chain isomorphism (4.6) preserves absolute Maslov grading as well.

Combining this with equation (4.5) and the previous fact that corresponding generators in $\mathcal{H}''$ and $\mathcal{H}'''$ have equal Maslov gradings, we conclude that the isomorphism from equation (4.4) shifts gradings by $n-1$. Then with the aid of equations (4.2) and (4.3), we arrive at the desired graded isomorphism equation (4.1). ∎

We turn now to Theorem 1.2, which states that τ_{top} of a Murasugi sum is maximal if and only if τ_{top} of each summand is maximal.

Proof of Theorem 1.2. By Proposition 2.10, we may take mirrors and prove the following statement for τ_{bot}: if L is a Murasugi sum of links L_1 and L_2 along minimal index Seifert surfaces, then $\tau_{\text{bot}}(L_i) = -g(L_i)$ for all $i \in \{1,2\}$ if and only if $\tau_{\text{bot}}(L) = -g(L)$.

We will continue from the previous proof, and re-use the same notation. Thanks to Corollary 2.9 and Proposition 2.10, we only need to prove that, for both $i = 1, 2$, the inclusion

$$\widetilde{SF}_{\mathcal{H}_i, S_i} \hookrightarrow \widetilde{CF}_{\mathcal{H}_i}$$

induces a non-zero map on homology if and only if the inclusion

$$\widetilde{SF}_{\mathcal{H}_1 * \mathcal{H}_2, S_1 * S_2} \hookrightarrow \widetilde{CF}_{\mathcal{H}_1 * \mathcal{H}_2}$$

induces a non-zero map on homology.

Thanks to equations (4.2) and (4.3), it is enough to prove the above for $(\mathcal{H}'', S')$, that is,

$$\begin{aligned} &\forall i\,(H_*(\widetilde{SF}_{\mathcal{H}''_i, S'_i}) \to H_*(\widetilde{CF}_{\mathcal{H}''_i}) \text{ is non-zero}) \\ &\iff H_*(\widetilde{SF}_{\mathcal{H}''_1 * \mathcal{H}''_2, S'_1 * S'_2}) \to H_*(\widetilde{CF}_{\mathcal{H}''_1 * \mathcal{H}''_2}) \text{ is non-zero.} \end{aligned} \tag{4.7}$$

Recall that we have nested subcomplexes

$$\widetilde{SF}_{\mathcal{H}'', S'} \hookrightarrow \widetilde{CF}^W_{\mathcal{H}''} \hookrightarrow \widetilde{CF}_{\mathcal{H}''}.$$

We claim the map $\widetilde{CF}^W_{\mathcal{H}''} \hookrightarrow \widetilde{CF}_{\mathcal{H}''}$ is injective on homology for $\mathcal{H}'' = \mathcal{H}''_1, \mathcal{H}''_2$, or $\mathcal{H}''_1 * \mathcal{H}''_2$. For each of the three diagrams, the homology of $\widetilde{CF}^W_{\mathcal{H}''}$ is isomorphic, up to a grading shift, to the homology of the $(n-1)$-times destabilized diagrams $\mathcal{H}'''_d$ (recall equation (4.5)); let ω denote its rank. By counting the number of basepoints, in each of the three cases, the homology of $\widetilde{CF}_{\mathcal{H}''}$ has rank $2^{n-1}\omega$. As before, the generators of $\widetilde{CF}_{\mathcal{H}''}$ can be represented as pairs $(\vec{a}, x^o)$ where $\vec{a} \in \{0,1\}^{n-1}$, and the differential is filtered with respect to $\vec{a}$. The associated graded complex of this filtration has 2^{n-1} summands, each isomorphic to $\widetilde{CF}^W_{\mathcal{H}''}$. By a spectral sequence argument, the homology of the quotient complex $\widetilde{CF}_{\mathcal{H}''}/\widetilde{CF}^W_{\mathcal{H}''}$ has rank at most $(2^{n-1}-1)\omega$. Therefore, in the exact triangle

$$\begin{array}{ccc} & H_*(\widetilde{CF}_{\mathcal{H}''}) & \\ \nearrow & & \searrow \\ H_*(\widetilde{CF}^W_{\mathcal{H}''}) & \longleftarrow & H_*(\widetilde{CF}_{\mathcal{H}''}/\widetilde{CF}^W_{\mathcal{H}''}) \end{array}$$

the three terms have ranks ω, $2^{n-1}\omega$, and at most $(2^{n-1}-1)\omega$, which implies that the map $H_*(\widetilde{CF}^W_{\mathcal{H}''}) \to H_*(\widetilde{CF}_{\mathcal{H}''})$ is injective.

Thanks to this, instead of equation (4.7), it is enough to prove

$$\begin{aligned} &\forall i\,(H_*(\widetilde{SF}_{\mathcal{H}''_i, S'_i}) \to H_*(\widetilde{CF}^W_{\mathcal{H}''_i}) \text{ is non-zero}) \\ &\iff H_*(\widetilde{SF}_{\mathcal{H}''_1 * \mathcal{H}''_2, S'_1 * S'_2}) \to H_*(\widetilde{CF}^W_{\mathcal{H}''_1 * \mathcal{H}''_2}) \text{ is non-zero,} \end{aligned}$$

which follows from equation (4.4). ∎

Remark 4.1. We remark that one direction of the theorem (maximality of τ_{top} of a Murasugi sum implies maximality for its summands) could be deduced from the fact that maximality of τ_{top} is preserved under taking subsurfaces of a minimal index Seifert surfaces. The latter fact is a consequence of a bound satisfied by τ_{top} for cobordisms between links, analogous to [13, Theorem 1].

Acknowledgments. This article started almost fifteen years ago, but was placed on hiatus multiple times due to a variety of reasons. We are grateful to Robert Lipshitz, Chuck Livingston, Yi Ni, Peter Ozsváth, and Zoltán Szabó for many helpful conversations about this paper at various points in the past decade. We would also like to thank the referee for many helpful comments and corrections.

Funding. Zhechi Cheng was supported from NSFC grant No. 12126101, NSF grants DMS-1609148, DMS-1564172 and Swedish Research Council under grant No. 2016-06596, Matthew Hedden was supported from NSF grants DMS-0706979, DMS-0906258, CAREER DMS-1150872, DMS-1709016, DMS-2104664 and an Alfred P. Sloan Research Fellowship and Sucharit Sarkar was supported from Clay Research Fellowship and NSF grants CAREER DMS-1350037, CAREER DMS-1643401, and DMS-1905717.

References

[1] J. Able and M. Hirasawa, Construction and decomposition of knots by Murasugi sums of Seifert surfaces. 2021, arXiv:2112.00297

[2] J. Baldwin and D. S. Vela-Vick, A note on the knot Floer homology of fibered knots. *Algebr. Geom. Topol.* **18** (2018), no. 6, 3669–3690 Zbl 1408.57012 MR 3868231

[3] A. Beliakova, A simplification of combinatorial link Floer homology. *J. Knot Theory Ramifications* **19** (2010), no. 2, 125–144 Zbl 1194.57017 MR 2647050

[4] A. Cavallo, The concordance invariant tau in link grid homology. *Algebr. Geom. Topol.* **18** (2018), no. 4, 1917–1951 Zbl 1422.57014 MR 3797061

[5] D. Gabai, The Murasugi sum is a natural geometric operation. In *Low-dimensional topology (San Francisco, Calif., 1981)*, pp. 131–143, Contemp. Math. 20, Amer. Math. Soc., Providence, RI, 1983 Zbl 0524.57004 MR 718138

[6] D. Gabai, The Murasugi sum is a natural geometric operation. II. In *Combinatorial methods in topology and algebraic geometry (Rochester, N.Y., 1982)*, pp. 93–100, Contemp. Math. 44, Amer. Math. Soc., Providence, RI, 1985 Zbl 0584.57003 MR 813105

[7] E. Giroux and N. Goodman, On the stable equivalence of open books in three-manifolds. *Geom. Topol.* **10** (2006), 97–114 Zbl 1100.57013 MR 2207791

[8] M. Hedden, On knot Floer homology and cabling. *Algebr. Geom. Topol.* **5** (2005), 1197–1222 Zbl 1086.57014 MR 2171808

[9] M. Hedden, *On knot Floer homology and cabling*. New York, NY, 2005 MR 2707267

[10] M. Hedden, Some remarks on cabling, contact structures, and complex curves. In *Proceedings of Gökova Geometry–Topology Conference 2007*, pp. 49–59, Gökova Geometry/Topology Conference (GGT), Gökova, 2008 Zbl 1187.57005 MR 2509749

[11] M. Hedden, On knot Floer homology and cabling. II. *Int. Math. Res. Not. IMRN* (2009), no. 12, 2248–2274 Zbl 1172.57008 MR 2511910

[12] M. Hedden, A. Juhász, and S. Sarkar, On sutured Floer homology and the equivalence of Seifert surfaces. *Algebr. Geom. Topol.* **13** (2013), no. 1, 505–548 Zbl 1272.57008 MR 3116378

[13] M. Hedden and K. Raoux, Knot Floer homology and relative adjunction inequalities. *Selecta Math. (N.S.)* **29** (2023), no. 1, article no. 7 Zbl 1507.57012 MR 4507976

[14] M. Hedden and L. Watson, On the geography and botany of knot Floer homology. *Selecta Math. (N.S.)* **24** (2018), no. 2, 997–1037 Zbl 1432.57027 MR 3782416

[15] A. Juhász, Floer homology and surface decompositions. *Geom. Topol.* **12** (2008), no. 1, 299–350 Zbl 1167.57005 MR 2390347

[16] R. Lipshitz, A cylindrical reformulation of Heegaard Floer homology. *Geom. Topol.* **10** (2006), 955–1096 Zbl 1130.57035 MR 2240908

[17] C. Manolescu, P. Ozsváth, and S. Sarkar, A combinatorial description of knot Floer homology. *Ann. of Math. (2)* **169** (2009), no. 2, 633–660 Zbl 1179.57022 MR 2480614

[18] K. Murasugi, On the genus of the alternating knot. I, II. *J. Math. Soc. Japan* **10** (1958), 94–105, 235–248 Zbl 0106.16701 MR 99664

[19] K. Murasugi, On a certain subgroup of the group of an alternating link. *Amer. J. Math.* **85** (1963), 544–550 Zbl 0117.17201 MR 157375

[20] W. Neumann and L. Rudolph, Unfoldings in knot theory. *Math. Ann.* **278** (1987), no. 1-4, 409–439 Zbl 0675.57010 MR 909235

[21] Y. Ni, A note on knot Floer homology of links. *Geom. Topol.* **10** (2006), 695–713 Zbl 1140.53038 MR 2240902

[22] Y. Ni, Sutured Heegaard diagrams for knots. *Algebr. Geom. Topol.* **6** (2006), 513–537 Zbl 1103.57021 MR 2220687

[23] P. Ozsváth and Z. Szabó, Knot Floer homology and the four-ball genus. *Geom. Topol.* **7** (2003), 615–639 Zbl 1037.57027 MR 2026543

[24] P. Ozsváth and Z. Szabó, Holomorphic disks and genus bounds. *Geom. Topol.* **8** (2004), 311–334 Zbl 1056.57020 MR 2023281

[25] P. Ozsváth and Z. Szabó, Holomorphic disks and knot invariants. *Adv. Math.* **186** (2004), no. 1, 58–116 Zbl 1062.57019 MR 2065507

[26] P. Ozsváth and Z. Szabó, Holomorphic disks and three-manifold invariants: properties and applications. *Ann. of Math. (2)* **159** (2004), no. 3, 1159–1245 Zbl 1081.57013 MR 2113020

[27] P. Ozsváth and Z. Szabó, Holomorphic disks and topological invariants for closed three-manifolds. *Ann. of Math. (2)* **159** (2004), no. 3, 1027–1158 Zbl 1073.57009 MR 2113019

[28] P. Ozsváth and Z. Szabó, Knot Floer homology, genus bounds, and mutation. *Topology Appl.* **141** (2004), no. 1-3, 59–85 Zbl 1052.57012 MR 2058681

[29] P. Ozsváth and Z. Szabó, Holomorphic disks, link invariants and the multi-variable Alexander polynomial. *Algebr. Geom. Topol.* **8** (2008), no. 2, 615–692 Zbl 1144.57011 MR 2443092

[30] P. Ozsváth and Z. Szabó, Algebras with matchings and knot Floer homology. 2019, arXiv:1912.01657

[31] P. S. Ozsváth, A. I. Stipsicz, and Z. Szabó, *Grid homology for knots and links*. Mathematical Surveys and Monographs 208, American Mathematical Society, Providence, RI, 2015 Zbl 1348.57002 MR 3381987

[32] J. A. Rasmussen, *Floer homology and knot complements.* Ph.D. Thesis, Harvard University, Cambridge, MA, 2003 MR 2704683

[33] L. Rudolph, Isolated critical points of mappings from $\mathbf{R}^4$ to $\mathbf{R}^2$ and a natural splitting of the Milnor number of a classical fibered link. I. Basic theory; examples. *Comment. Math. Helv.* **62** (1987), no. 4, 630–645 Zbl 0626.57020 MR 920062

[34] J. R. Stallings, Constructions of fibred knots and links. In *Algebraic and geometric topology (Proc. Sympos. Pure Math., Stanford Univ., Stanford, Calif., 1976),* Part 2, pp. 55–60, Proc. Sympos. Pure Math., XXXII, American Mathematical Society, Providence, RI, 1978 Zbl 0394.57007 MR 520522

[35] A. Thompson, A note on Murasugi sums. *Pacific J. Math.* **163** (1994), no. 2, 393–395 Zbl 0809.57003 MR 1262303

Received 25 February 2022.

Zhechi Cheng
School of Mathematics and Statistics, Wuhan University, #299 Ba Yi Road, Wuchang District, 430072 Wuhan, China; chengzhechi@gmail.com

Matthew Hedden
Department of Mathematics, Michigan State University, 619 Red Cedar Road, Wells Hall D325, East Lansing, MI 48824, USA; matthew.hedden@gmail.com

Sucharit Sarkar
Department of Mathematics, University of California, Los Angeles, 520 Portola Plaza, Box 95155, Los Angeles, CA 90095-1555, USA; sucharit.sarkar@gmail.com